Supplementary Information For:

Two birds with one arrow: functionalized Al(III) MOF acts as a fluorometric sensor of dopamine in bio-fluids and recyclable catalyst for Biginelli reaction

Subhrajyoti Ghosh,[a] Nagarathinam Nagarjun,[b] Soutick Nandi,[ac] Amarajothi Dhakshinamoorthy,[b] and Shyam Biswas*[a]*

[a] *Department of Chemistry, Indian Institute of Technology Guwahati, 781039 Assam, India.*

[b] *School of Chemistry, Madurai Kamaraj University, Madurai, Tamil Nadu, 625021, India.*

[c] *Department of Applied Science, Ghani Khan Choudhury Institute of Engineering & Technology, Malda, 732141 West Bengal, India.*

*Corresponding author. Tel: 91-3612583309, Fax: 91-3612582349

E-mail address: sbiswas@iitg.ac.in, admguru@gmail.com

Materials and characterization methods:

All the chemicals except 5-boronoisophthalic acid were purchased from commercial sources and used without further purification. A Bruker Avance III 600 spectrometer was utilized for recording ^{1}H NMR and ^{13}C NMR spectra at 400 MHz and 100 MHz respectively. The mass spectrum (in ESI mode) was measured with an Agilent 6520 Q-TOF high-resolution mass spectrometer. Fourier transform infrared (FT-IR) spectroscopy data were recorded in the region 400-4000 cm^{-1} at room temperature with the Perkin Elmer Spectrum Two FT-IR spectrometer. The following indications were used to indicate the corresponding absorption bands: very strong (vs), strong (s), medium (m), weak (w), shoulder (sh) and broad (br). Thermogravimetric (TG) experiments were carried out with a heating rate of 5 °C min^{-1} under nitrogen atmosphere using a SDT Q600 thermogravimetric analyser. Powder X-ray diffraction (PXRD) instrument Rigaku Smartlab X-ray diffractometer (model TTRAX III) with Cu-Kα radiation (λ = 1.54056 Å), 50 kV of operating voltage and 100 mA of operating current was used for the collection of all PXRD data. Specific surface area for N_2 sorption was calculated on a Quantachrome Autosorb iQMP gas sorption analyser at -196 °C. FE-SEM images were collected with a Zeiss (Sigma 300) scanning electron microscope. The compound was activated at 100 °C for 12 h under dynamic vacuum. Fluorescence emission studies were performed at room temperature using a HORIBA JOBIN YVON Fluoromax-4 spectrofluorometer. Fluorescence lifetime measurements were performed by time correlated single-photon counting (TCSPC) method by an Edinburgh Instrument Life-Spec II instrument. The UV-Vis spectra were measured with a PerkinElmer Lambda 25 UV-Vis spectrometer.

Synthesis procedure of 5-boronoisophthalic acid linker:

This compound was synthesised according to previously reported procedure (Scheme S1).[1] 3,5-Dimethylphenylboronic acid (1 g, 6.7 mol) and NaOH (500 mg, 12.5 mol) were dissolved in *tert*-butanol/water (v/v = 1:1; 25 mL). The reaction mixture was heated to 50 °C under stirring condition. After that small portion (100 mg) of $KMnO_4$ were added to the solution. After few moments, colour of the solution changed from violet to brown. Then, the rest of $KMnO_4$ (6.5 g) was added and the temperature was set to 70 °C. At last, additional $KMnO_4$ (600 mg) was included. After 3 hours, the reaction was stopped and the excess $KMnO_4$ was reduced by the addition of $Na_2S_2O_3$ (100 mg) and filtered. The filtrate was concentrated to ~15 mL by evaporation and acidified to pH = 1 using concentrated HCl. After that, the white precipitate was collected by filtration and dried in a conventional oven. Yield: 885 mg (4.21 mmol, 63%). ^{1}H NMR (400 MHz, DMSO-d_6): δ = 8.61 (d, 2H), 8.50 (t, 1H), 8.43 (s, 2H) ppm ^{13}C NMR (100 MHz, DMSO-d_6): δ = 167.04, 139.14, 131.65, 130.43 ppm. ESI-MS (m/z): 209.0255 for $(M-H)^-$ ion (M = mass of 3,5-dimethylphenylboronic acid acid linker). Figures S1-S3 show the NMR and mass spectra of the synthesized 3,5-dimethylphenylboronic acid linker.

Scheme S1. Reaction scheme for the preparation of 5-boronoisophthalic acid linker.

Preparation of MOF (1′) suspension for the fluorescence sensing experiments:
The probe **1′** (3 mg) was taken in a 5 mL glass vial containing 3 mL HEPES buffer. For the sensing experiments in aqueous medium, HEPES buffer was replaced by Milli-Q water. Then, the suspension was sonicated for 15 min and kept it for overnight to make the suspension stable. During the fluorescence experiment, 100 µL of above-mentioned suspension of **1′** was added to 3000 µL of Milli-Q water/HEPES buffer in a quartz cuvette. All the fluorescence spectra were collected in the range of 290-420 nm by exciting the suspension at 280 nm. For competitive experiments, the solutions of the different competitive analytes (concentration = 10 mM) were added to the suspension of **1′** and spectra were collected in the same range.

Fluorescence detection of dopamine in human blood serum and urine samples:
From the vein of a healthy volunteer, 10 mL of blood sample was collected. The collected blood sample was then immediately centrifuged for 15 min at 3000 rpm speed in order to separate the blood cells. The light yellow coloured serum was collected by using a Pasteur pipette and it was diluted to 1000 times to its original concentration. After that, the serum was immediately stored at 0 °C. Thereafter, appropriate amount of free dopamine was added to human blood serum to make the dopamine concentration of 10 mM in the medium. After that, different volumes of dopamine-spiked human blood serum were introduced into the HEPES buffer suspension of the probe and fluorescence spectra were recorded.

The human urine sample of 10 mL was collected. Then, the urine sample was acidified with 500 µL of conc. HNO_3 and centrifuged at 3000 rpm for 15 min. The supernatant was collected and it was diluted to 100 times of its original concentration. Then, the dopamine concentration in the urine sample was made 10 mM after the addition of appropriate amount of free dopamine into the urine samples. Different volumes of this solution were used for dopamine detection in urine samples (λ_{ex} = 280 nm, λ_{em} = 350 nm).

General procedure for Biginelli reaction:

A reaction tube was charged with 25 mg of catalyst. Then, benzaldehyde (0.4 mmol), ethylacetoacetate (1 mmol) and urea (0.7 mmol) were added in a conventional catalytic reaction. Then, 0.1 mL of solvent was added to this combination and homogeneously mixed before it was placed in an oil bath maintained at 80 °C. Table 1 shows how long this reaction mixture was agitated for. GC-MS was used to track the development of the reaction. The reaction was quenched and the reaction tube was allowed to cool to room temperature when it had completed. The mixture was afterwards diluted with ethanol, filtered, and GC-MS examined to determine the final yield of the product. GC-MS and ^{1}H NMR were used to confirm the products. Reusability tests were carried out in a manner similar to that described above, with the exception of the addition of recovered catalyst obtained by filtration after the reaction, which was washed three times with fresh ethanol (5 mL) and dried at 100 °C for three hours.

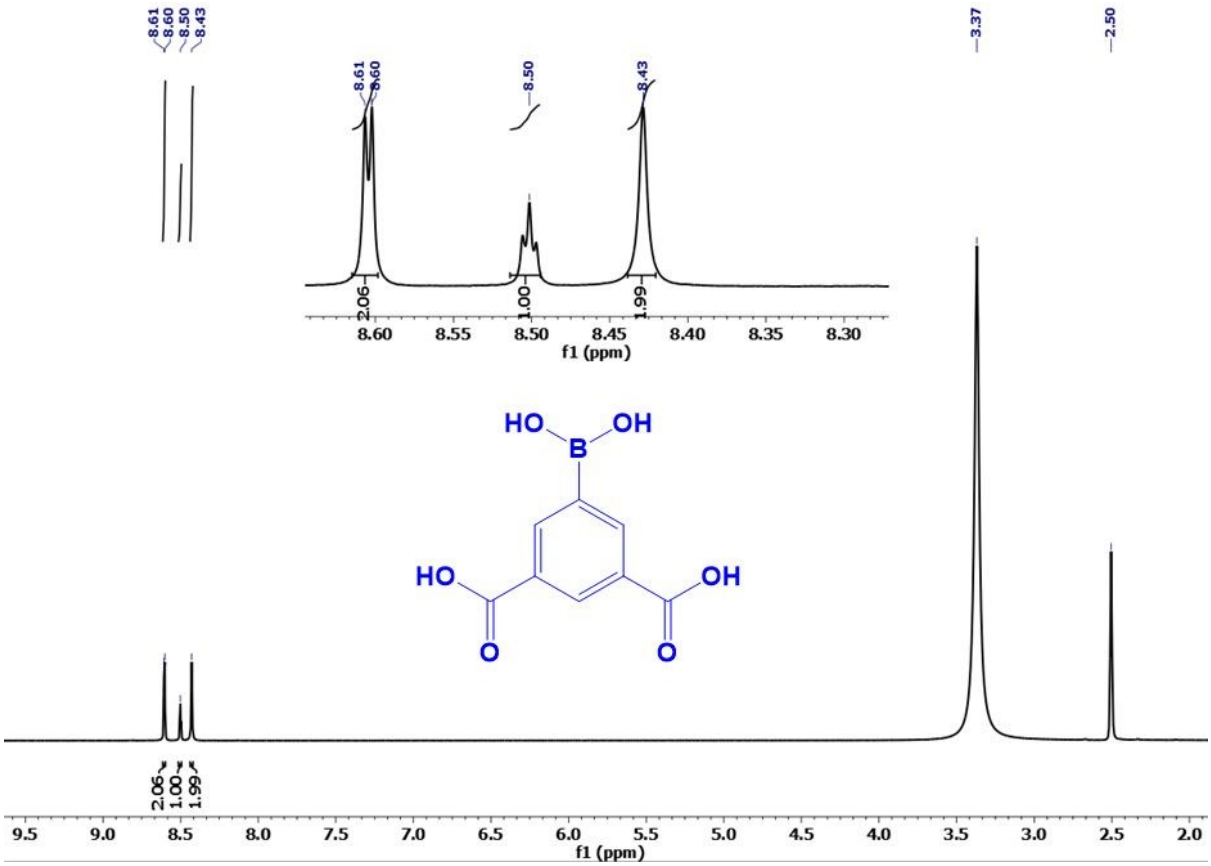

Fig. S1. ^{1}H NMR spectrum of 5-boronoisophthalic acid linker in DMSO-d_6.

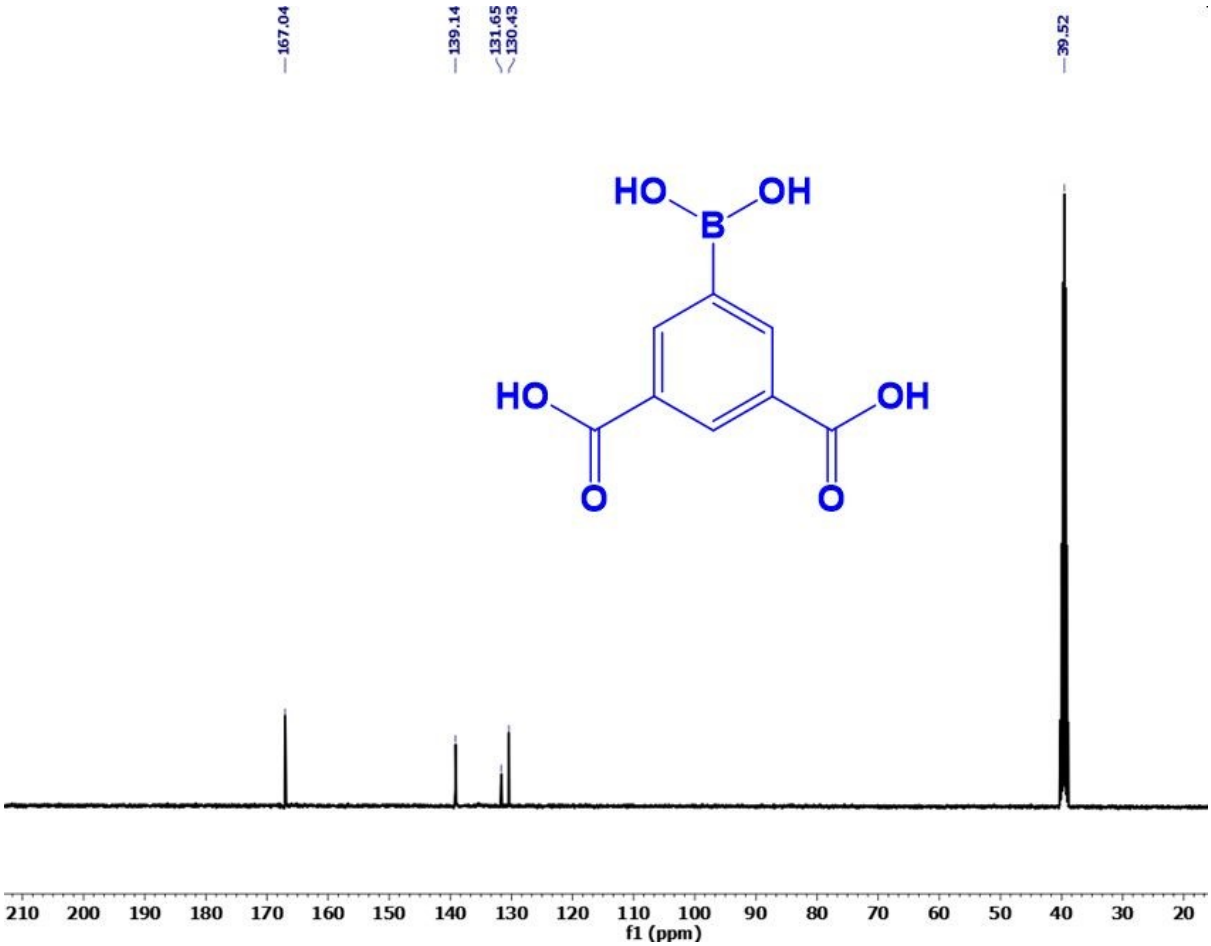

Fig. S2. ^{13}C NMR spectrum of 5-boronoisophthalic acid linker in DMSO-d_6.

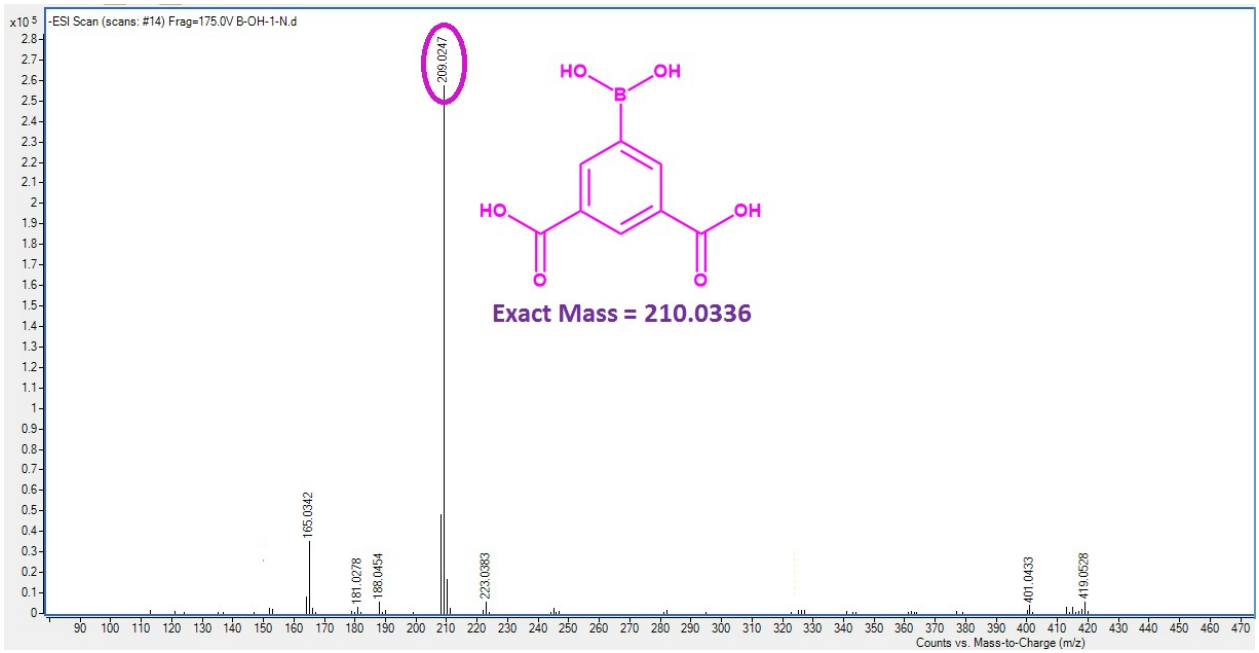

Fig. S3. ESI-MS spectrum of 5-boronoisophthalic acid linker measured in methanol. The spectrum shows m/z peak at 209.0255, which corresponds to $(M\text{-}H)^-$ ion (M = mass of 5-boronoisophthalic acid linker).

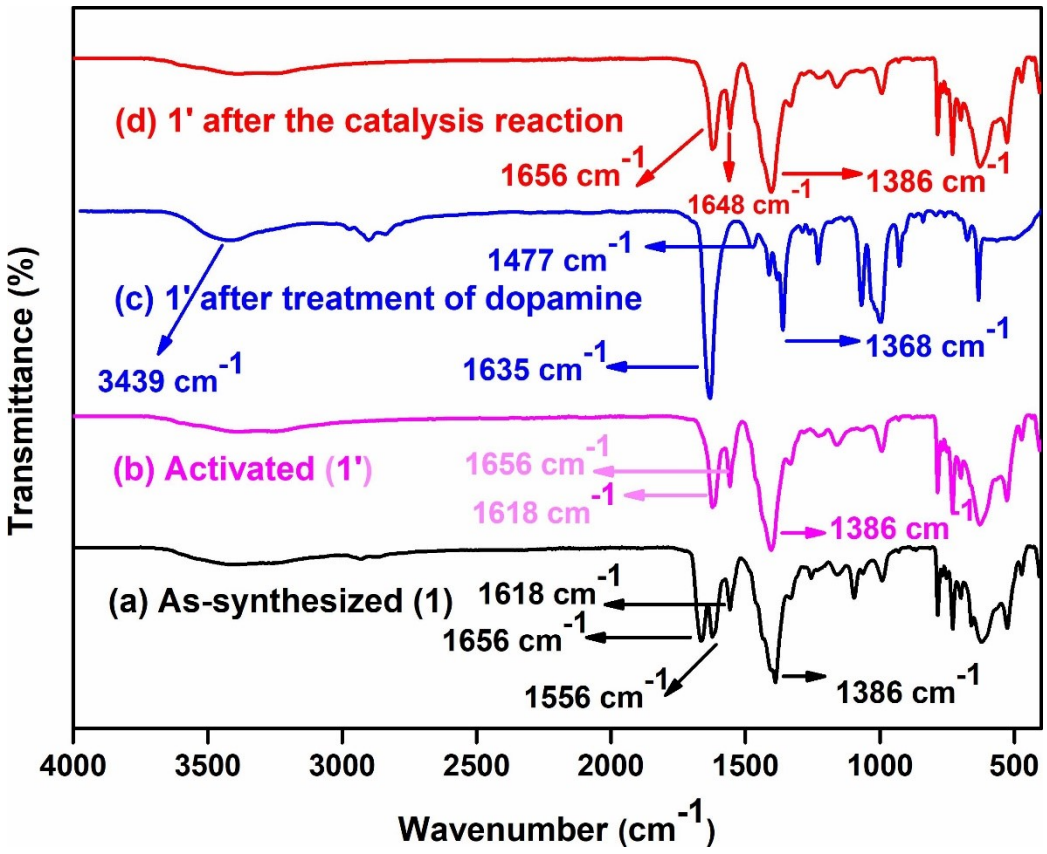

Fig. S4. FT-IR spectra of (a) as-synthesized **1**, (b) activated **1′** (c) **1′** after treatment of dopamine and (d) **1′** after catalysis reaction.

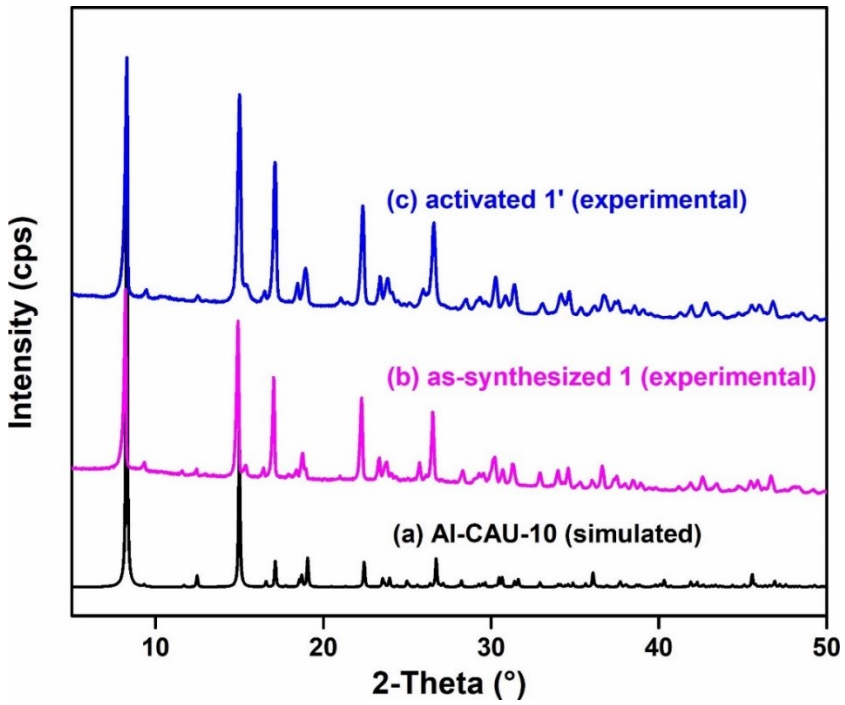

Fig. S5. PXRD patterns of (a) simulated Al-CAU-10 (black), (b) as-synthesized **1** (pink) and (c) activated **1′** (blue).

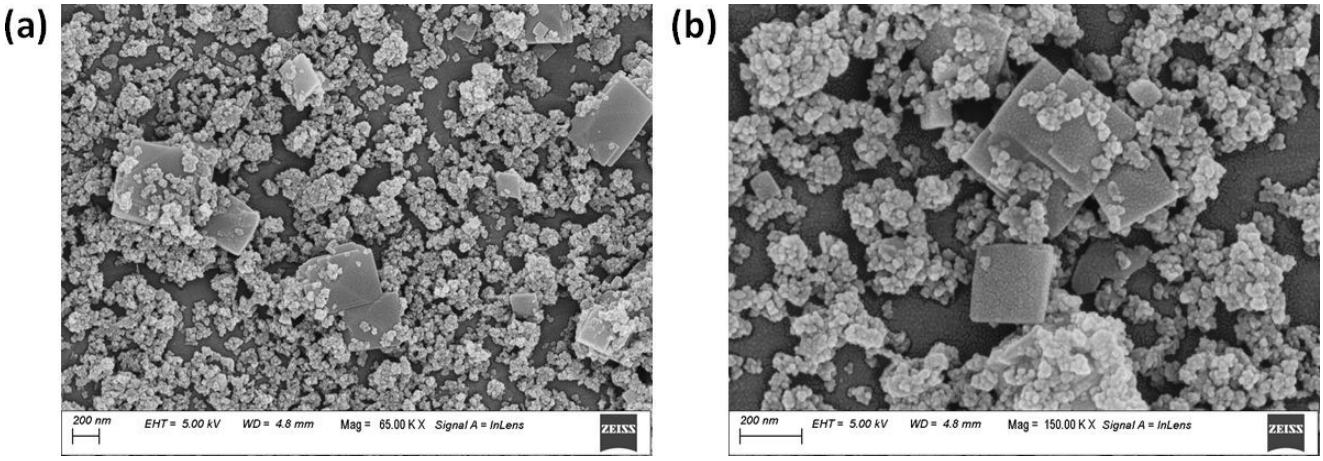

Fig. S6. FE-SEM images of (a) as-synthesized **1** and (b) activated **1′** after catalysis reaction.

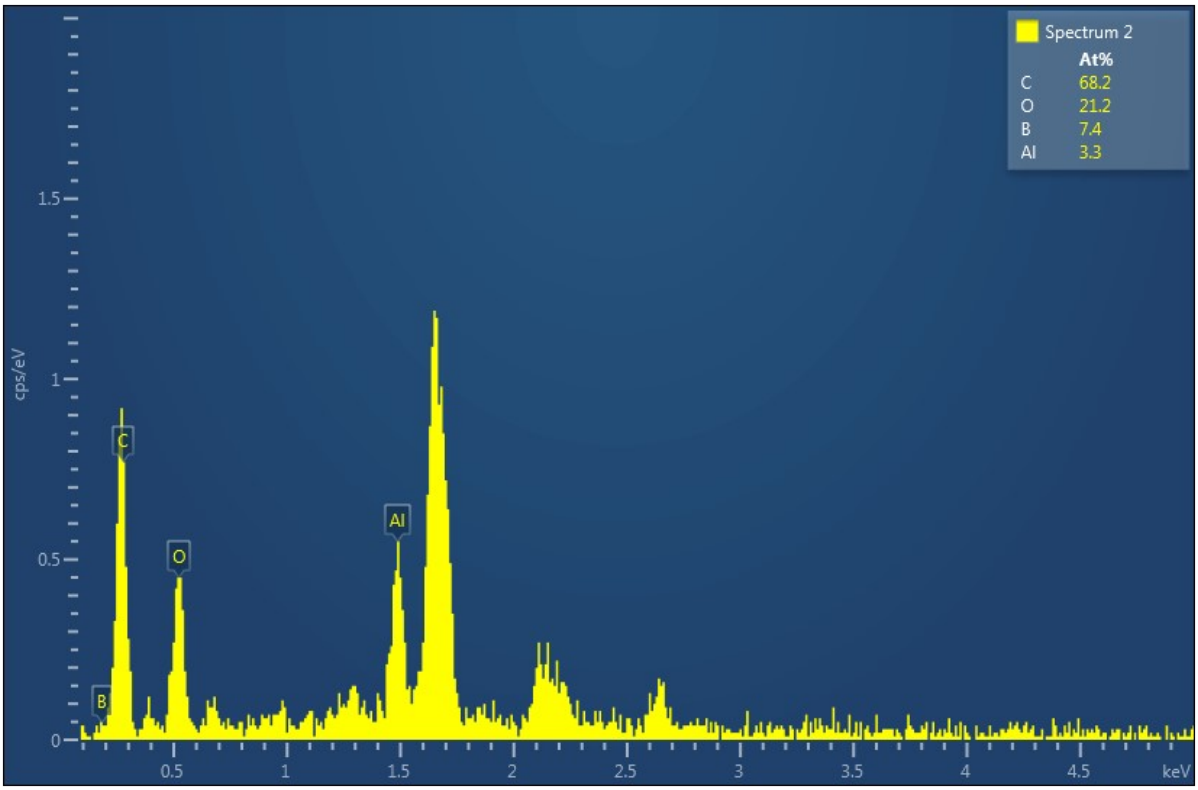

Fig. S7. EDX spectrum of **1′**.

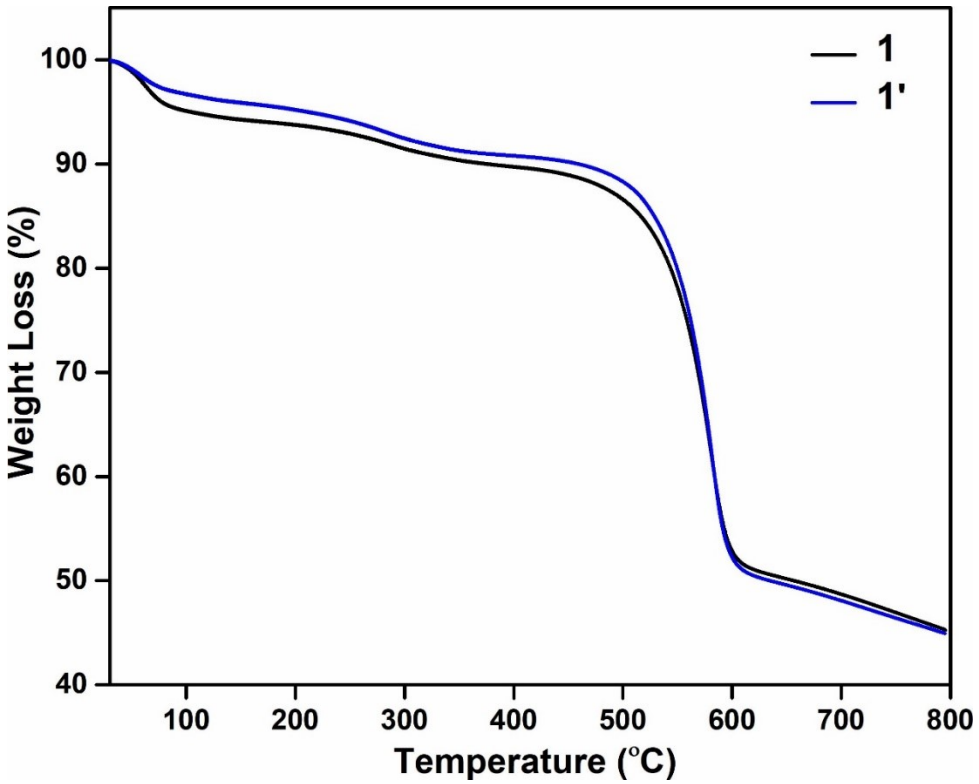

Fig. S8. Thermogravimetric analysis curves of as-synthesized **1** (black) and thermally activated **1′** (blue) recorded under N_2 atmosphere in the temperature range of 25-800 °C with a heating rate of 5 °C min^{-1}.

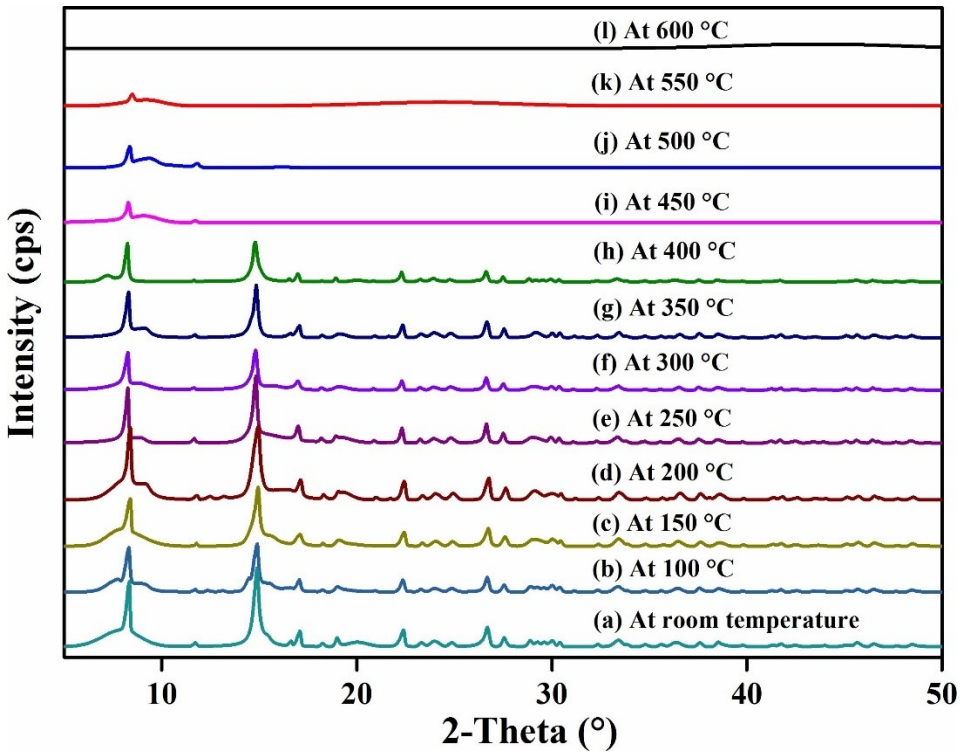

Fig. S9. Temperature dependent PXRD of **1′.**

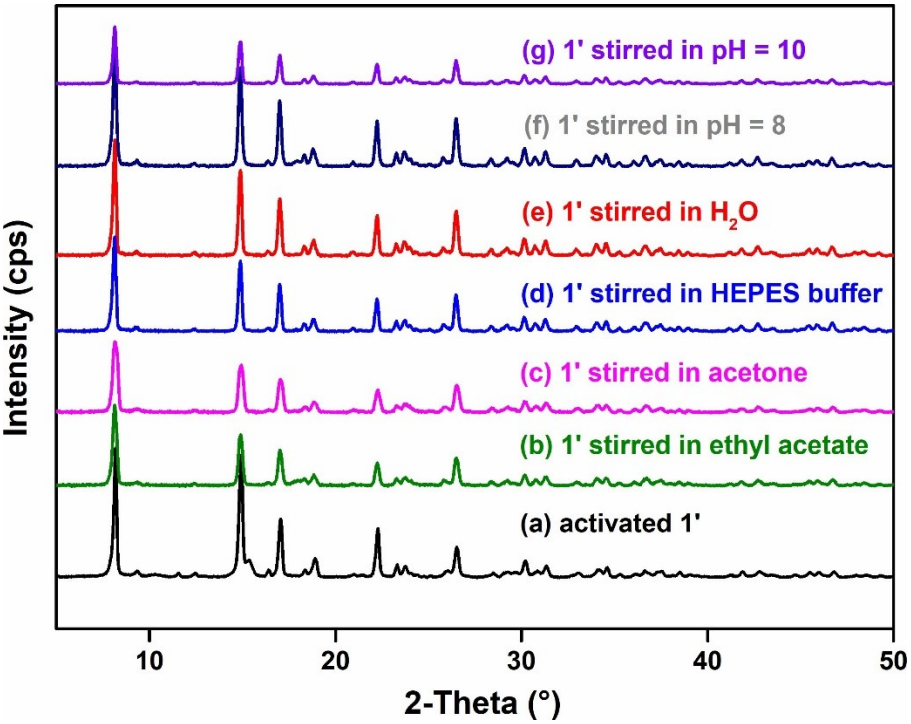

Fig. S10. PXRD patterns of **1′** in different forms: (a) activated **1′**, after stirred with (b) ethyl acetate (c) acetone (d) HEPES buffer, (e) H_2O (f) pH =8 and (g) pH =10 for 12 h.

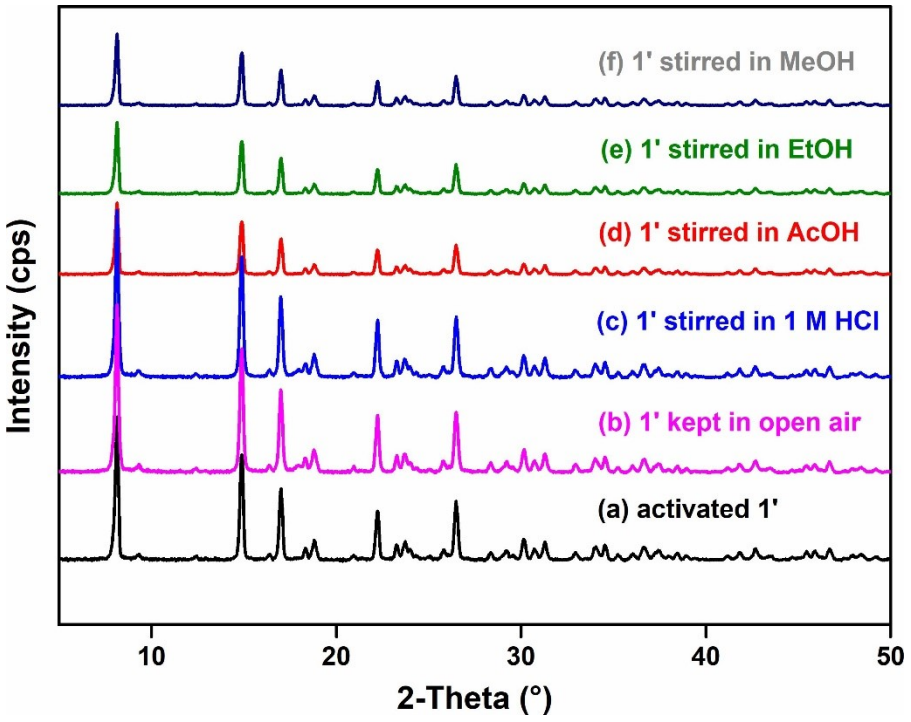

Fig. S11. PXRD patterns of **1′** in different forms: (a) activated **1′**, (b) kept in open air, after stirred with (c) 1M HCl (d) AcOH (e) EtOH and (f) MeOH for 12 h.

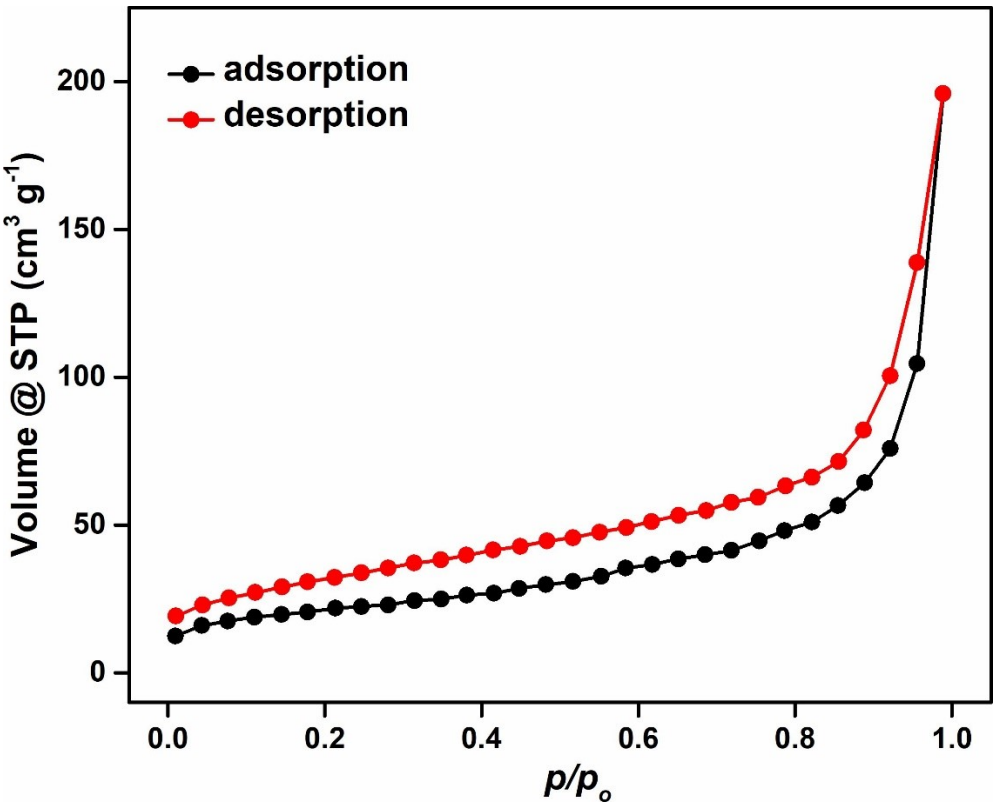

Fig. S12. N_2 adsorption (black circles) and desorption (red circles) isotherms of thermally activated **1′** recorded at –196 °C.

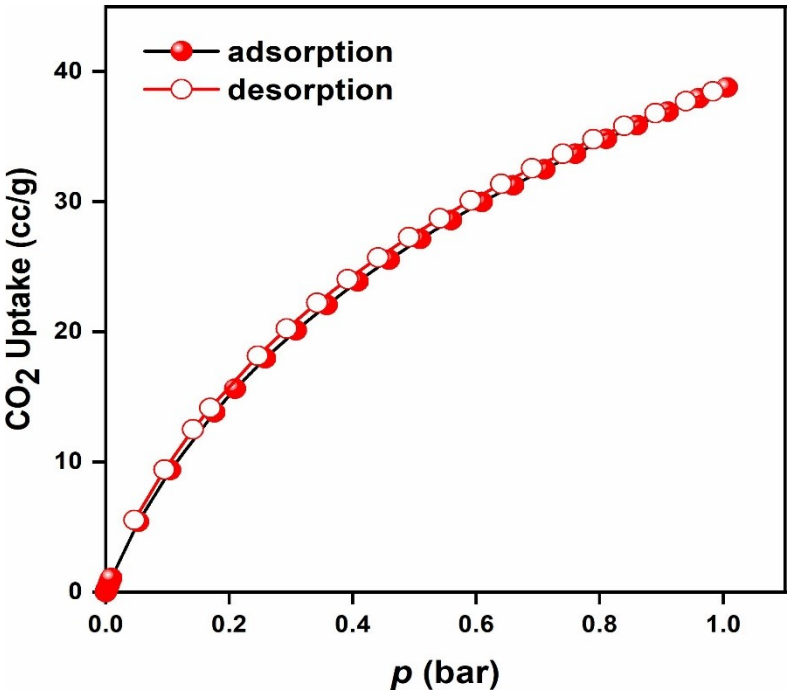

Fig. S13. CO_2 adsorption (solid circles) and desorption (hollow circles) isotherms of thermally activated **1′** recorded at 0 °C.

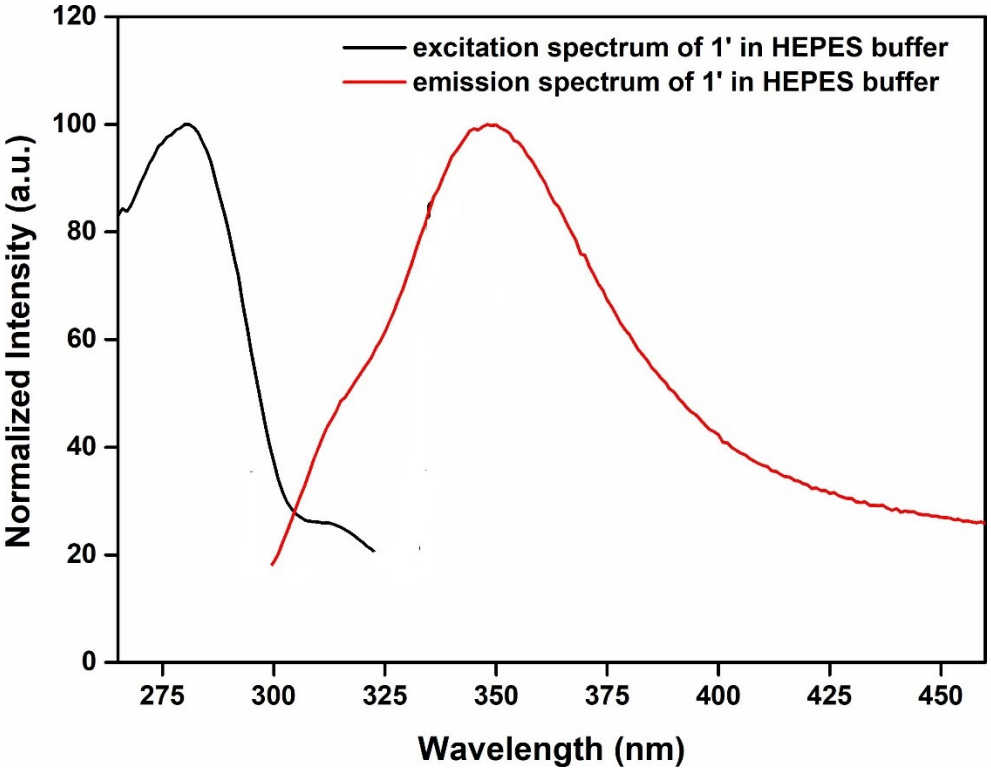

Fig. S14. Excitation (black) and emission (red) spectra of **1′** in HEPES buffer medium.

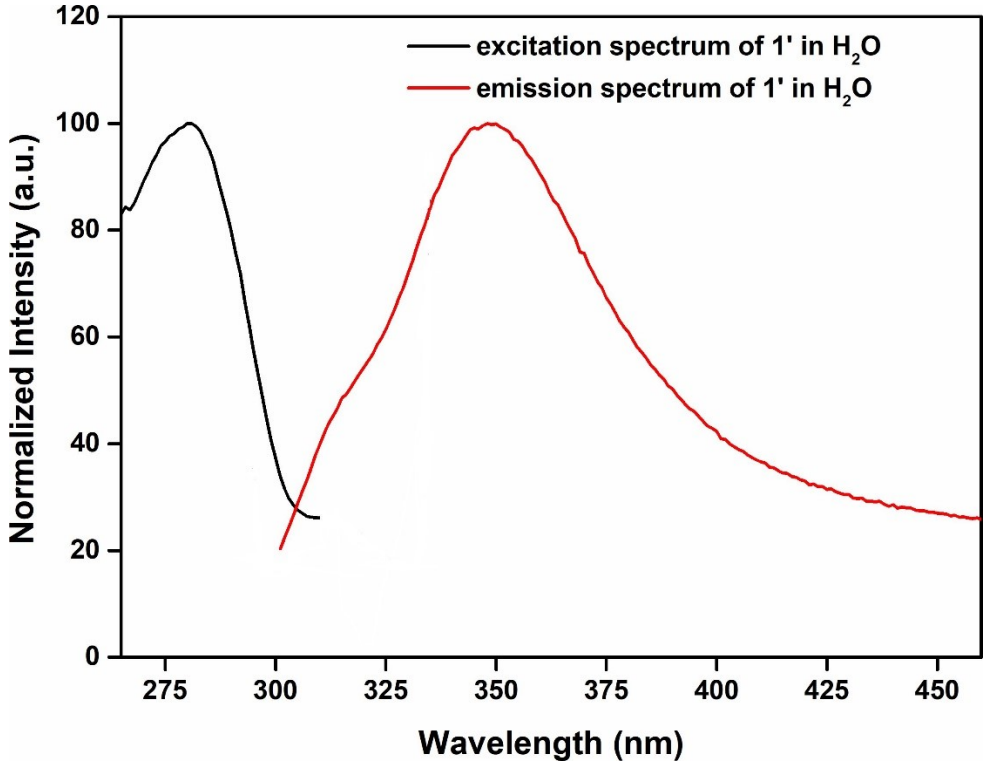

Fig. S15. Excitation (black) and emission (red) spectra of **1′** in aqueous medium.

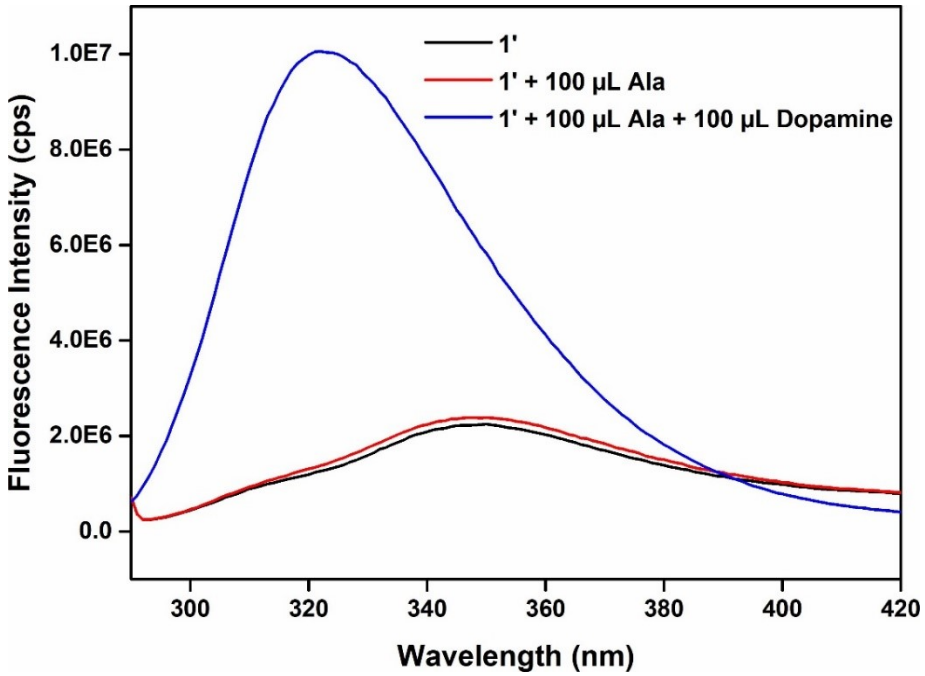

Fig. S16. Increment in fluorescence emission intensity of the suspension of **1′** in HEPES buffer medium after addition of 100 µL of 10 mM aqueous dopamine solution in presence of 100 µL of 10 mM aqueous solution of alanine (Ala).

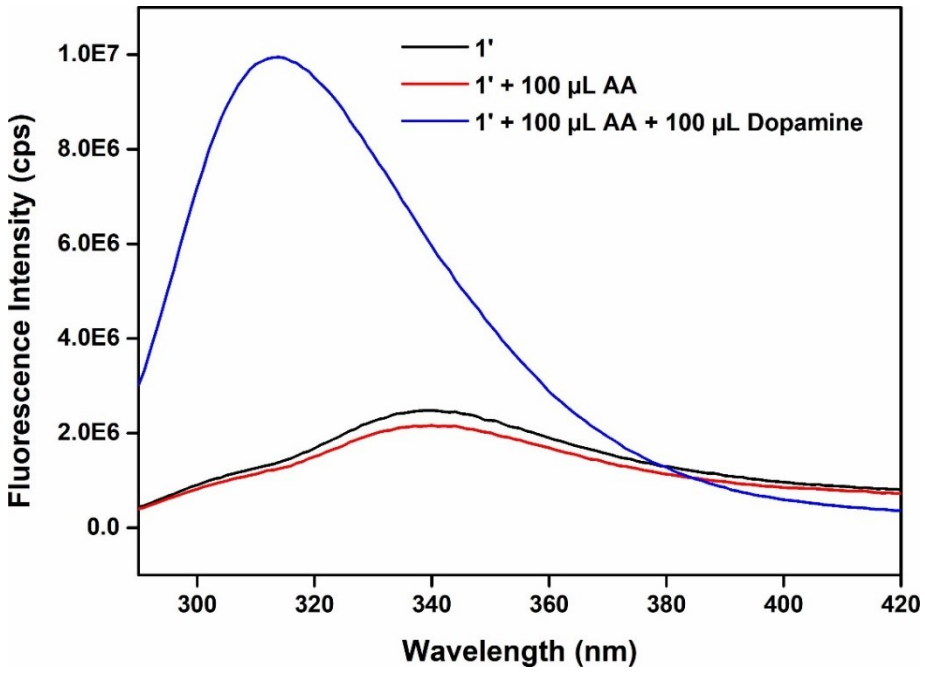

Fig. S17. Increment in fluorescence emission intensity of the suspension of **1′** in HEPES buffer medium after addition of 100 µL of 10 mM aqueous dopamine solution in presence of 100 µL of 10 mM aqueous solution of ascorbic acid (AA).

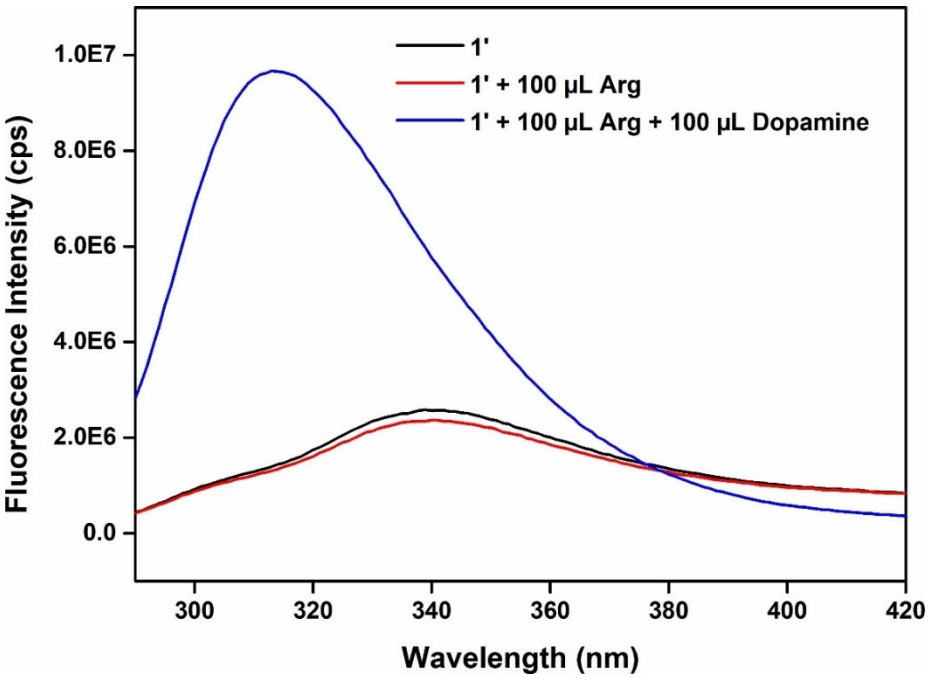

Fig. S18. Increment in fluorescence emission intensity of the suspension of **1′** in HEPES buffer medium after addition of 100 µL of 10 mM aqueous dopamine solution in presence of 100 µL of 10 mM aqueous solution of arginine (Arg).

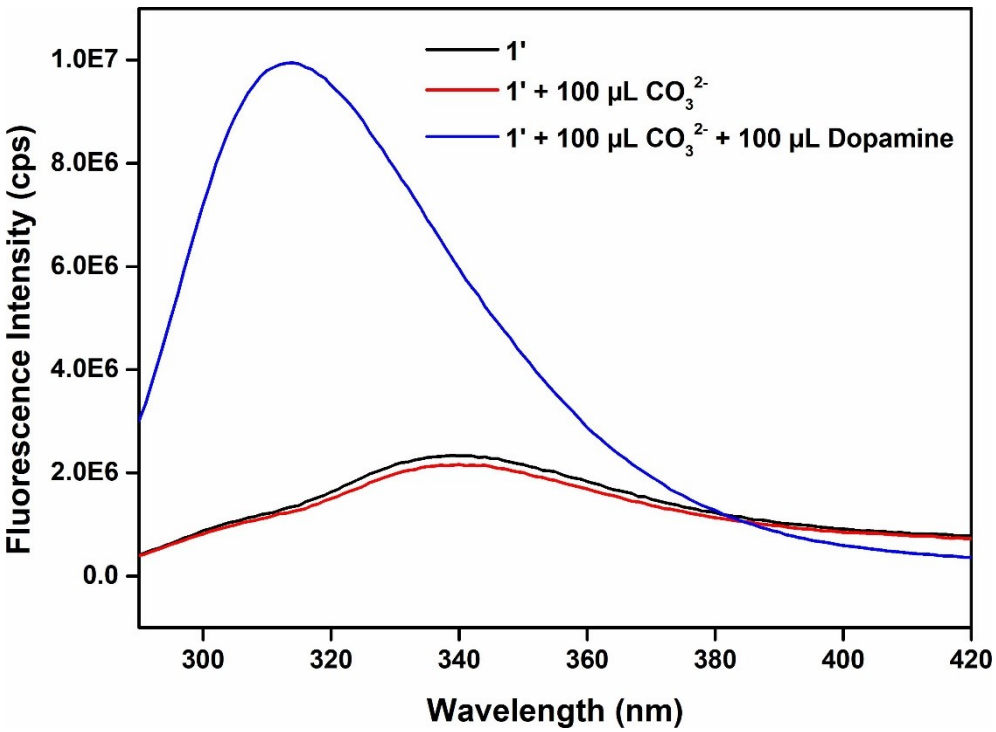

Fig. S19. Increment in fluorescence emission intensity of the suspension of **1′** in HEPES buffer medium after addition of 100 µL of 10 mM aqueous dopamine solution in presence of 100 µL of 10 mM aqueous solution of CO_3^{2-}.

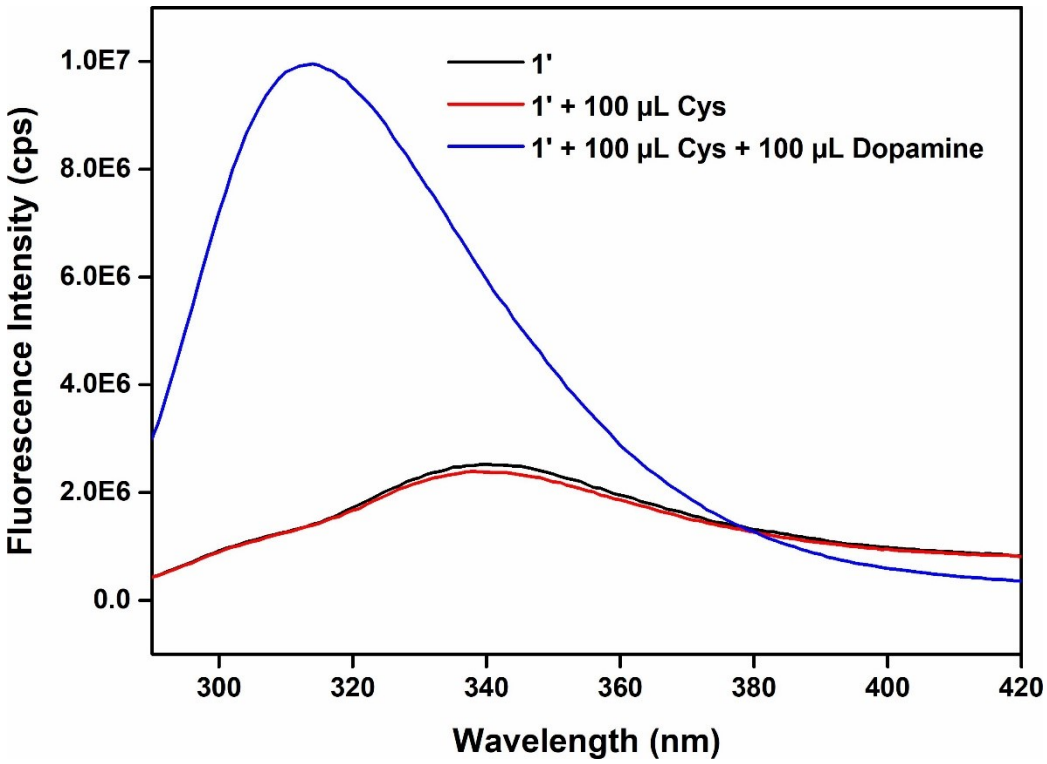

Fig. S20. Increment in fluorescence emission intensity of the suspension of **1′** in HEPES buffer medium after addition of 100 µL of 10 mM aqueous dopamine solution in presence of 100 µL of 10 mM aqueous solution of cysteine (Cys).

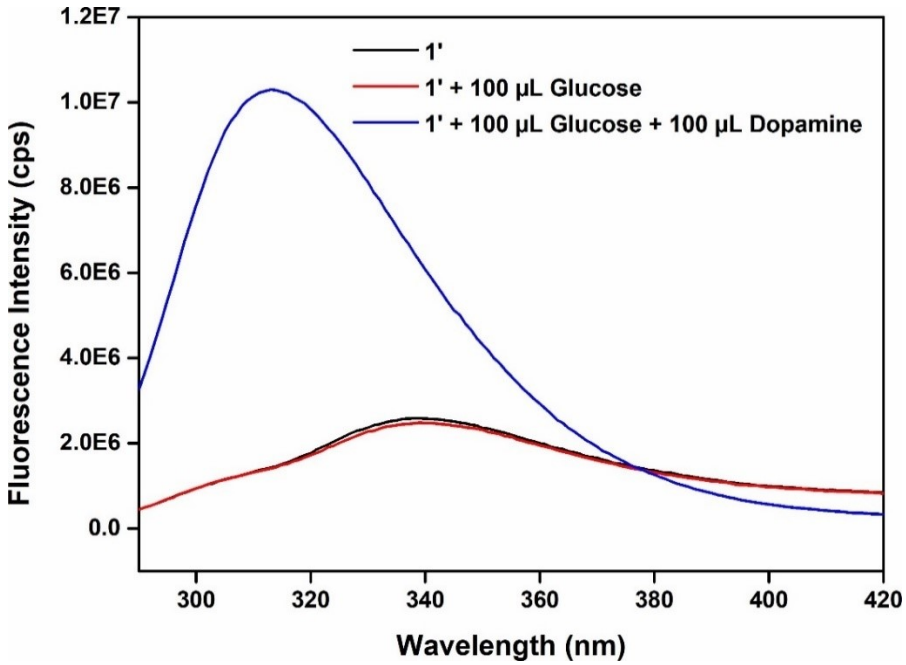

Fig. S21. Increment in fluorescence emission intensity of the suspension of **1′** in HEPES buffer medium after addition of 100 µL of 10 mM aqueous dopamine solution in presence of 100 µL of 10 mM aqueous solution of glucose.

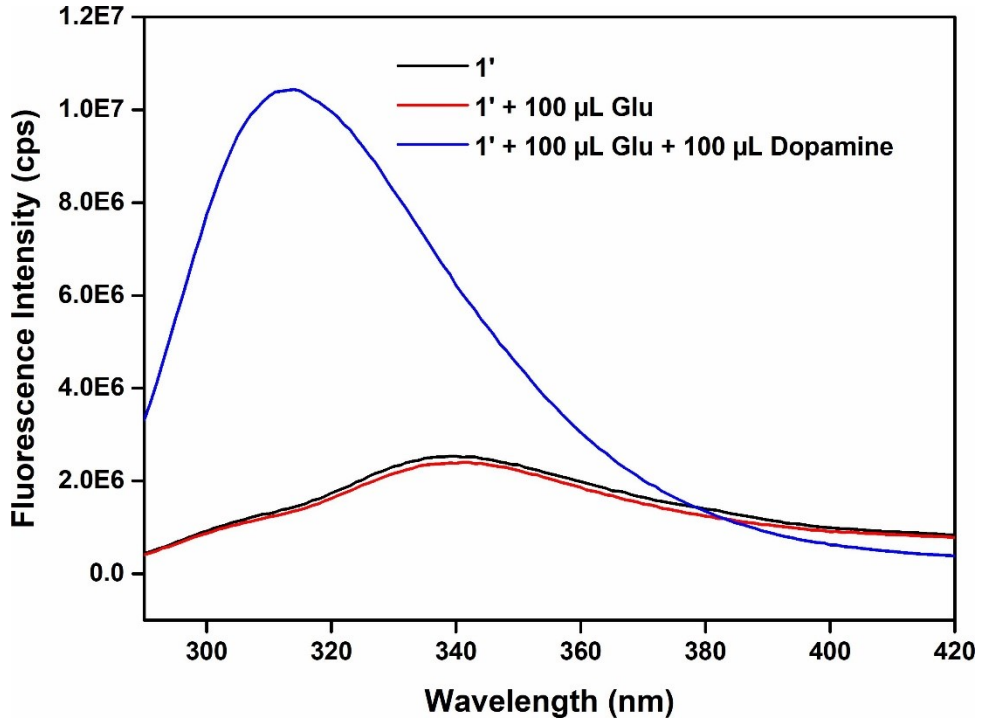

Fig. S22. Increment in fluorescence emission intensity of the suspension of **1′** in HEPES buffer medium after addition of 100 µL of 10 mM aqueous dopamine solution in presence of 100 µL of 10 mM aqueous solution of glutathione (Glu).

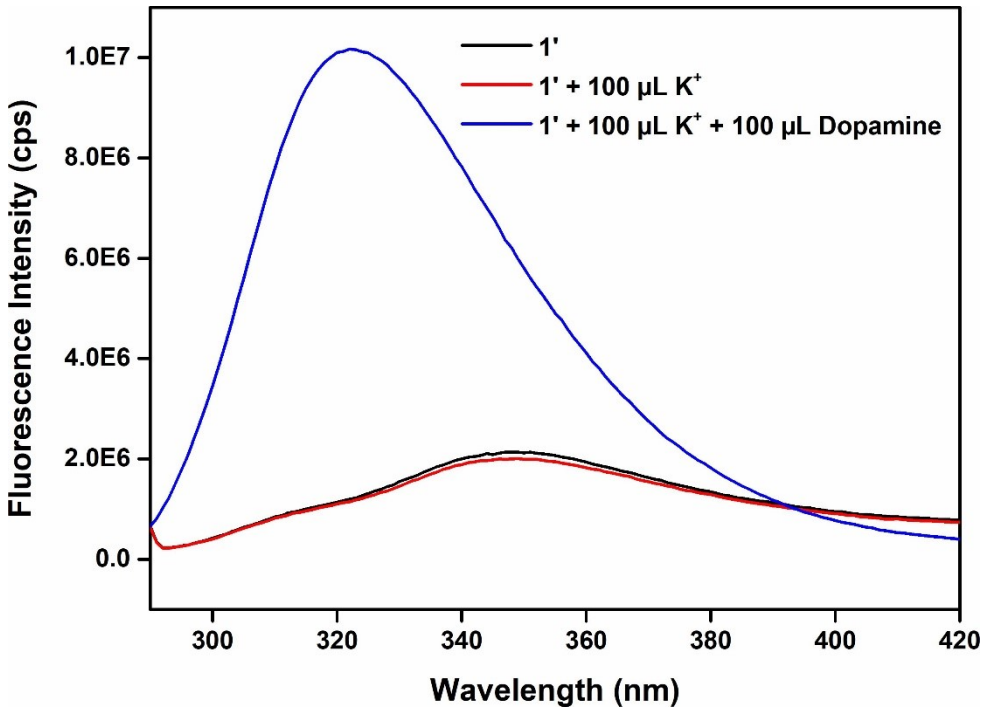

Fig. S23. Increment in fluorescence emission intensity of the suspension of **1′** in HEPES buffer medium after addition of 100 µL of 10 mM aqueous dopamine solution in presence of 100 µL of 10 mM aqueous solution of K^+.

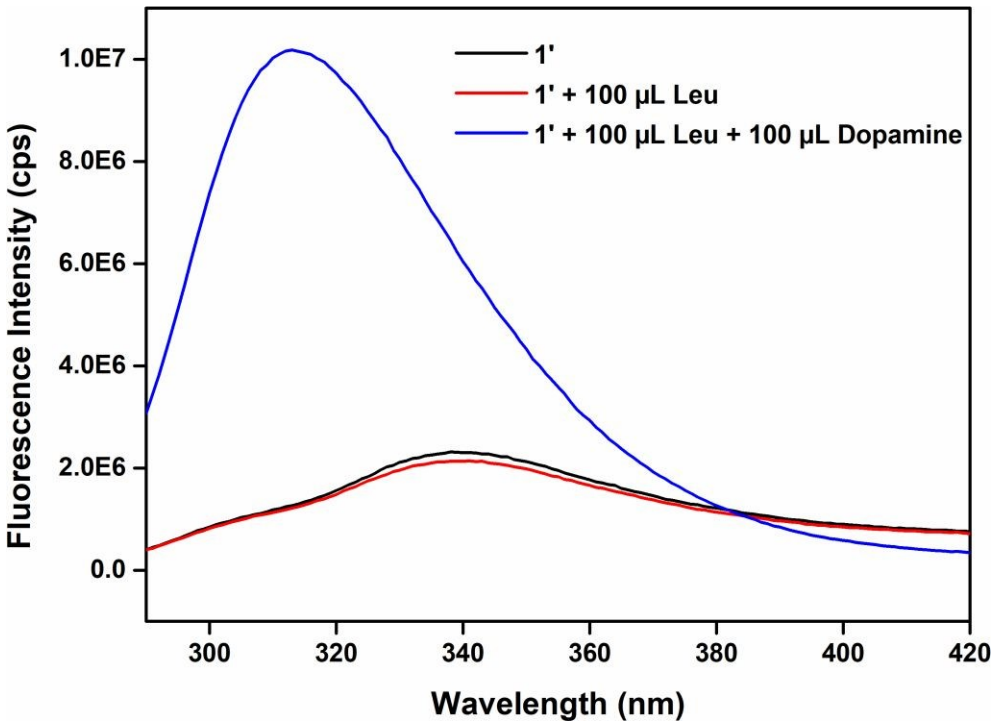

Fig. S24. Increment in fluorescence emission intensity of the suspension of **1′** in HEPES buffer medium after addition of 100 µL of 10 mM aqueous dopamine solution in presence of 100 µL of 10 mM aqueous solution of leucine (Leu).

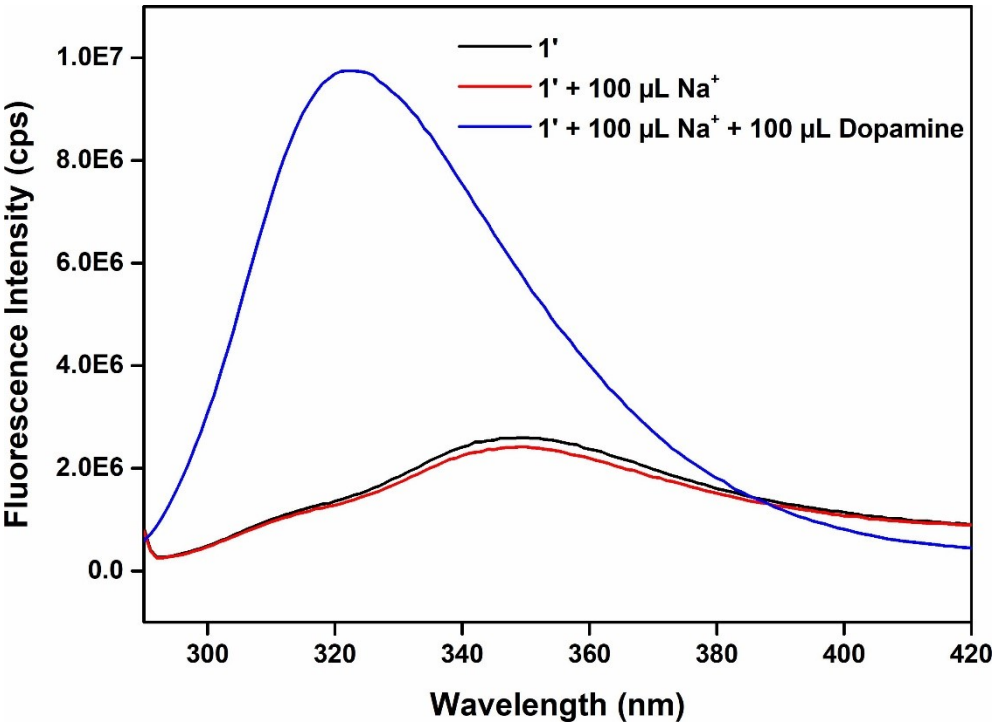

Fig. S25. Increment in fluorescence emission intensity of the suspension of **1′** in HEPES buffer medium after addition of 100 µL of 10 mM aqueous dopamine solution in presence of 100 µL of 10 mM aqueous solution of Na^+.

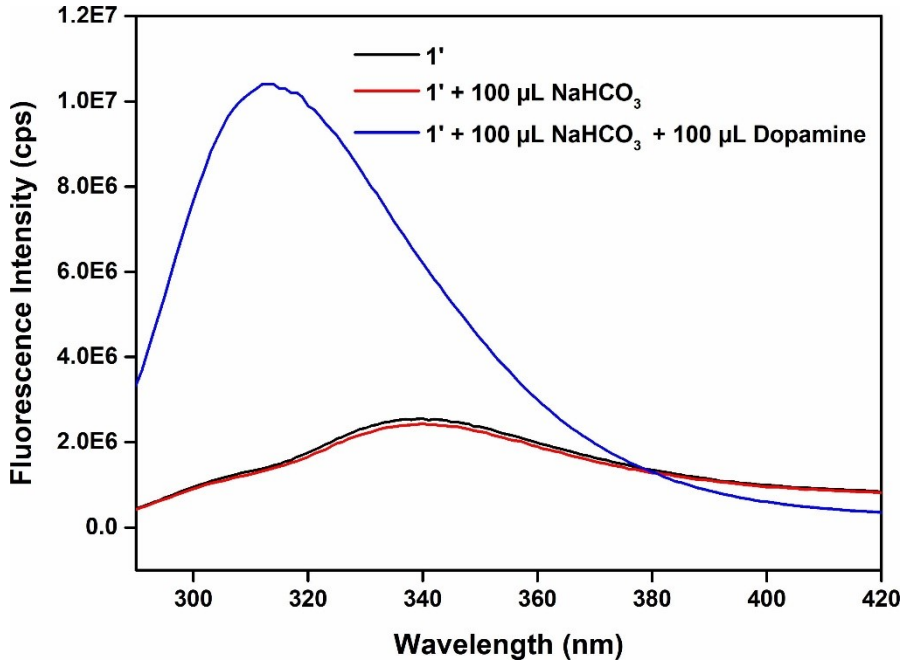

Fig. S26. Increment in fluorescence emission intensity of the suspension of **1′** in HEPES buffer medium after addition of 100 µL of 10 mM aqueous dopamine solution in presence of 100 µL of 10 mM aqueous solution of $NaHCO_3$.

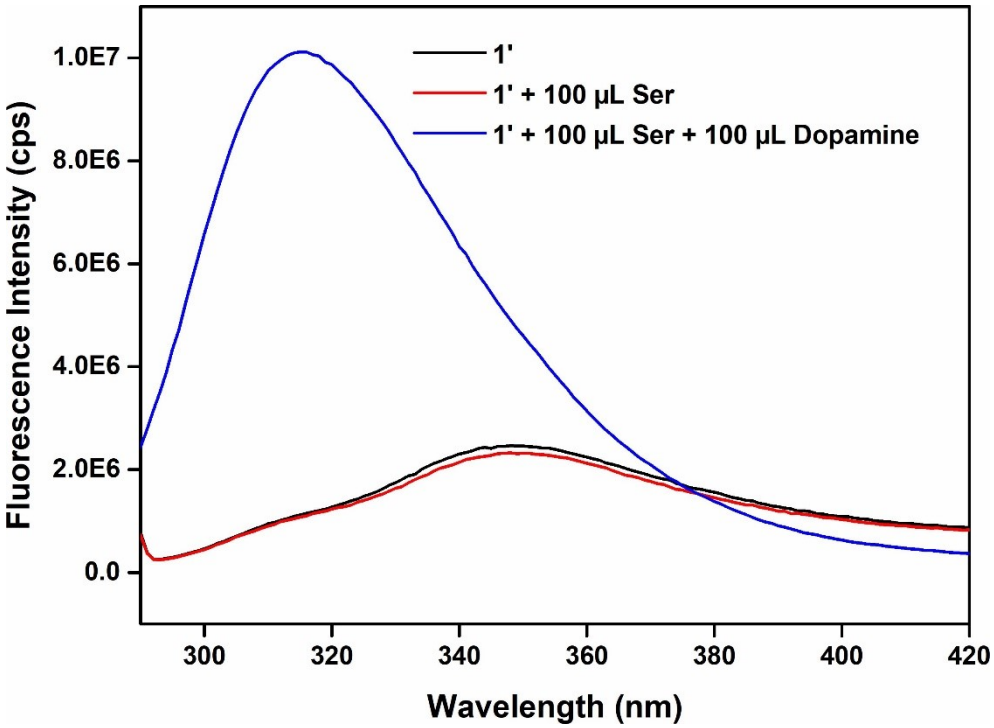

Fig. S27. Increment in fluorescence emission intensity of the suspension of **1′** in HEPES buffer medium after addition of 100 µL of 10 mM aqueous dopamine solution in presence of 100 µL of 10 mM aqueous solution of serine (Ser).

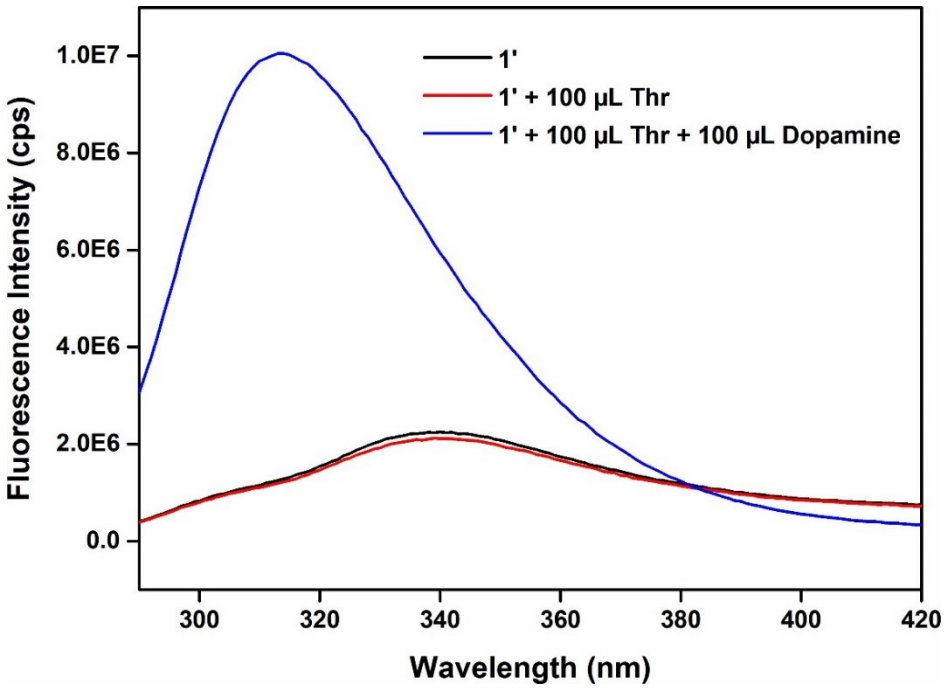

Fig. S28. Increment in fluorescence emission intensity of the suspension of **1′** in HEPES buffer medium after addition of 100 µL of 10 mM aqueous dopamine solution in presence of 100 µL of 10 mM aqueous solution of threonine (Thr).

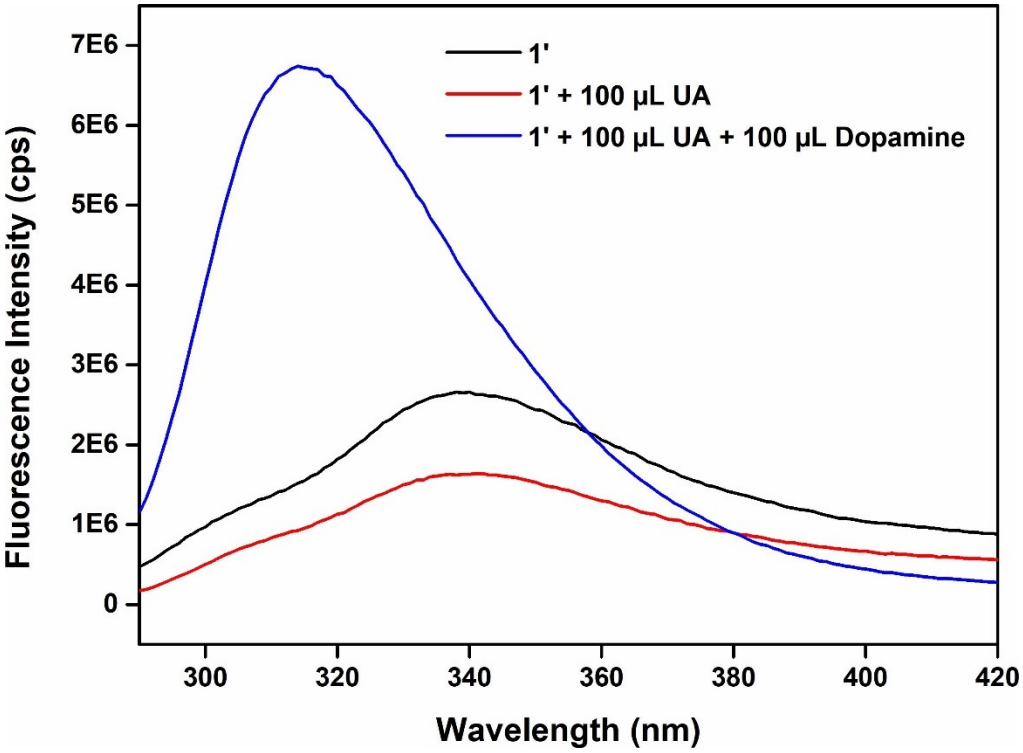

Fig. S29. Increment in fluorescence emission intensity of the suspension of **1′** in HEPES buffer medium after addition of 100 µL of 10 mM aqueous dopamine solution in presence of 100 µL of 10 mM aqueous solution of uric acid (UA).

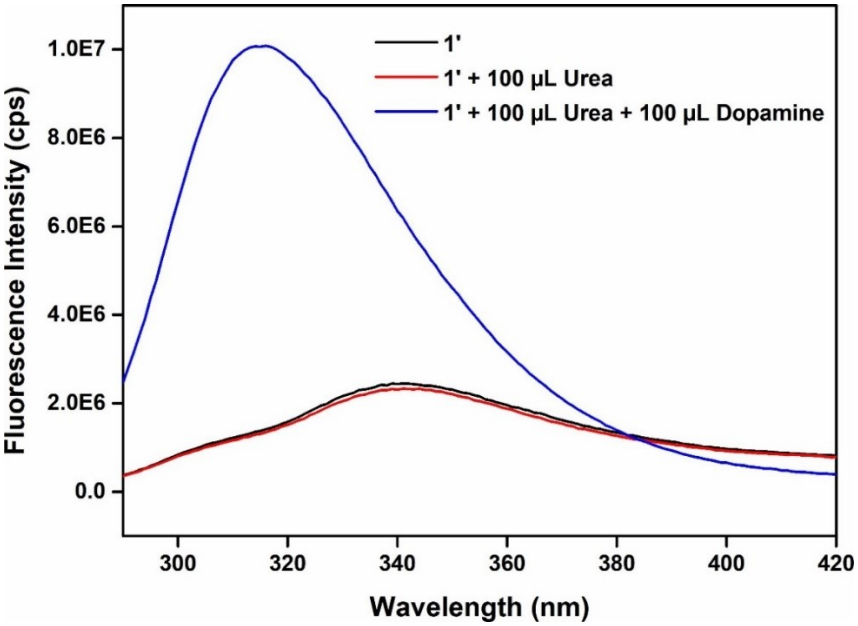

Fig. S30. Increment in fluorescence emission intensity of the suspension of **1′** in HEPES buffer medium after addition of 100 µL of 10 mM aqueous dopamine solution in presence of 100 µL of 10 mM aqueous solution of urea.

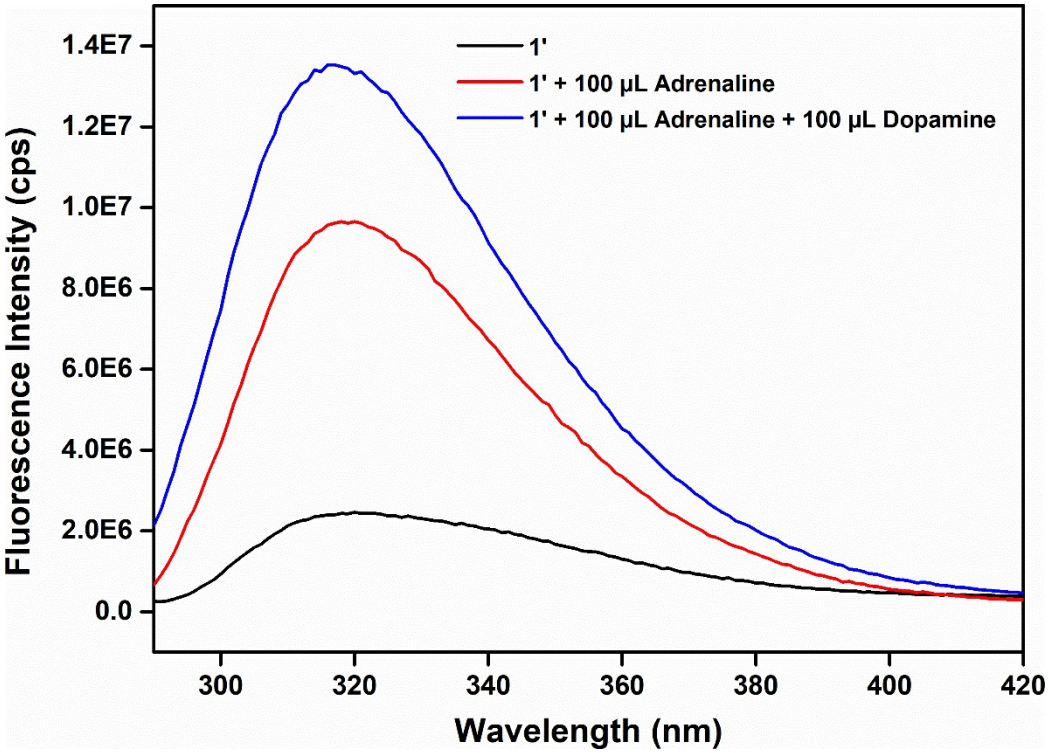

Fig. S31. Increment in fluorescence emission intensity of the suspension of **1′** in HEPES buffer medium after addition of 100 µL of 10 mM aqueous dopamine solution in presence of 100 µL of 10 mM aqueous solution of adrenaline.

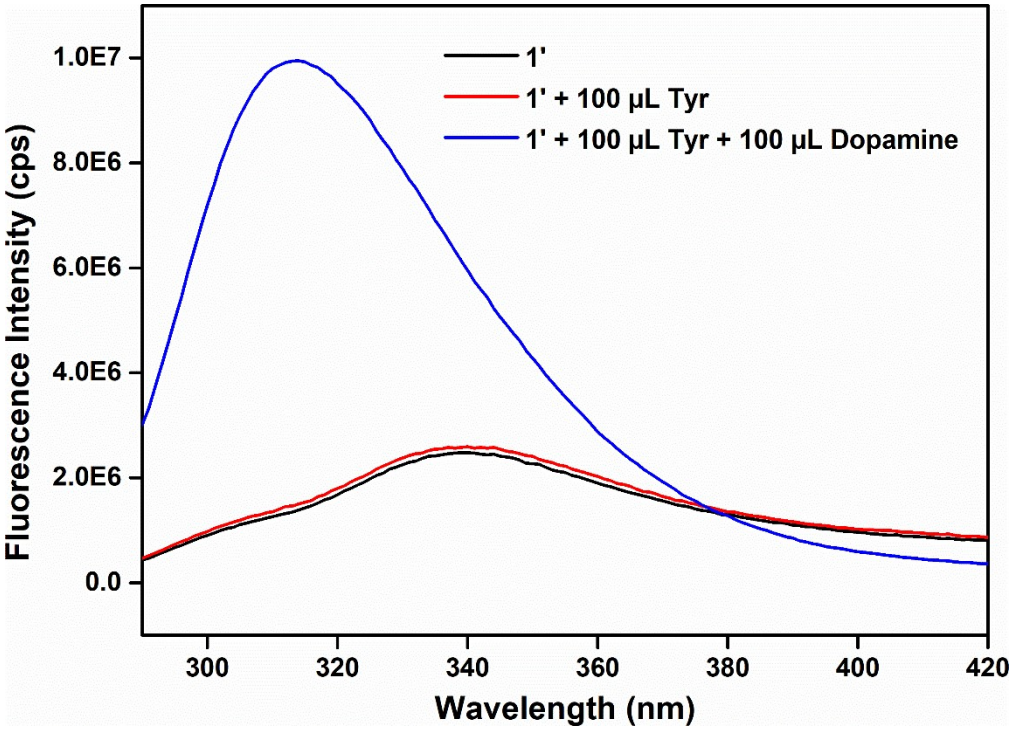

Fig. S32. Increment in fluorescence emission intensity of the suspension of **1′** in HEPES buffer medium after addition of 100 µL of 10 mM aqueous dopamine solution in presence of 100 µL of 10 mM aqueous solution of tyrosine (Tyr).

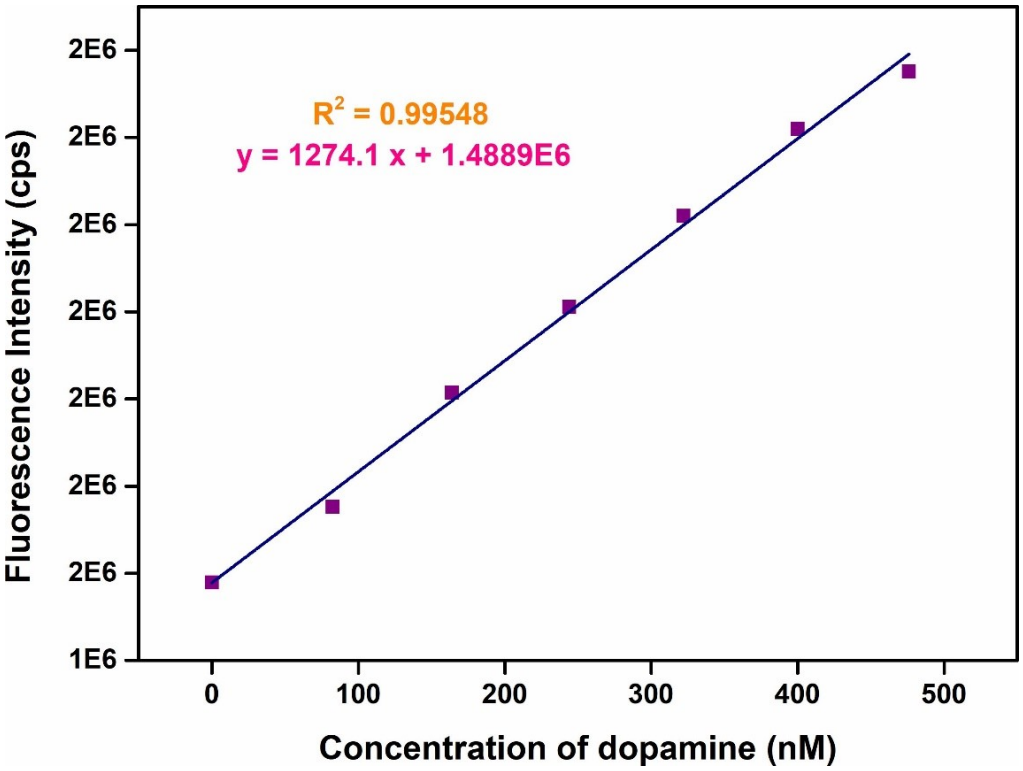

Fig. S33. Change in the fluorescence emission intensity of **1′** in HEPES buffer as a function of concentration of dopamine.

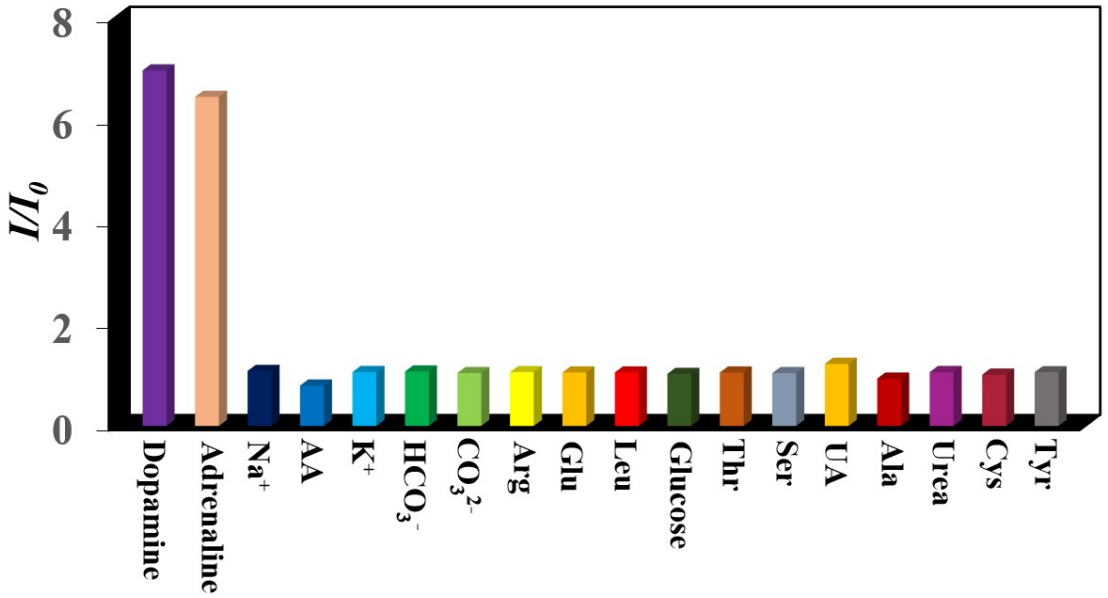

Fig. S34. Fluorescence changes of **1′** after adding 100 μL of 10 mM different competitive analytes into the aqueous suspension of **1′** (λ_{ex} = 280 nm, λ_{em} = 350 nm).

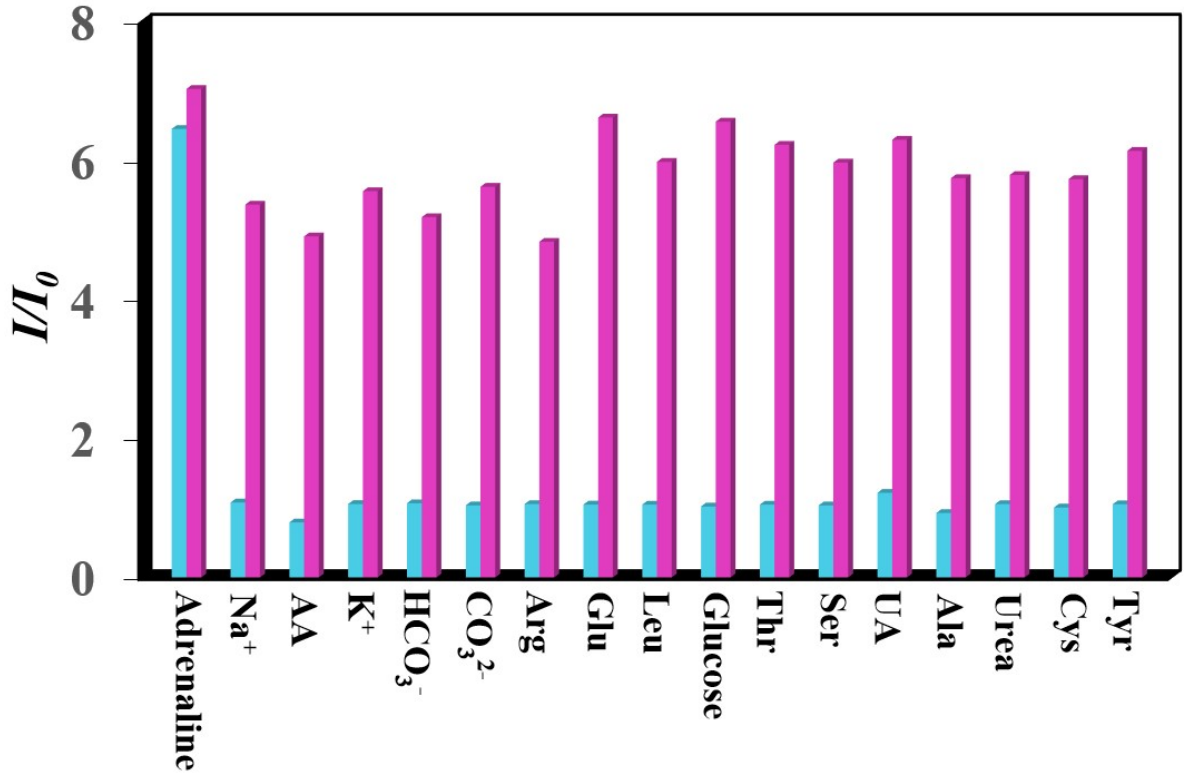

Fig. S35. Relative fluorescence changes of **1′** after adding 100 μL of 10 mM dopamine solution in presence of 100 μL of 10 mM different competitive analytes into an aqueous suspension of **1′** (λ_{ex} = 280 nm, λ_{em} = 350 nm) (blue bars for competitive analytes and pink bars are for competitive analyte + dopamine).

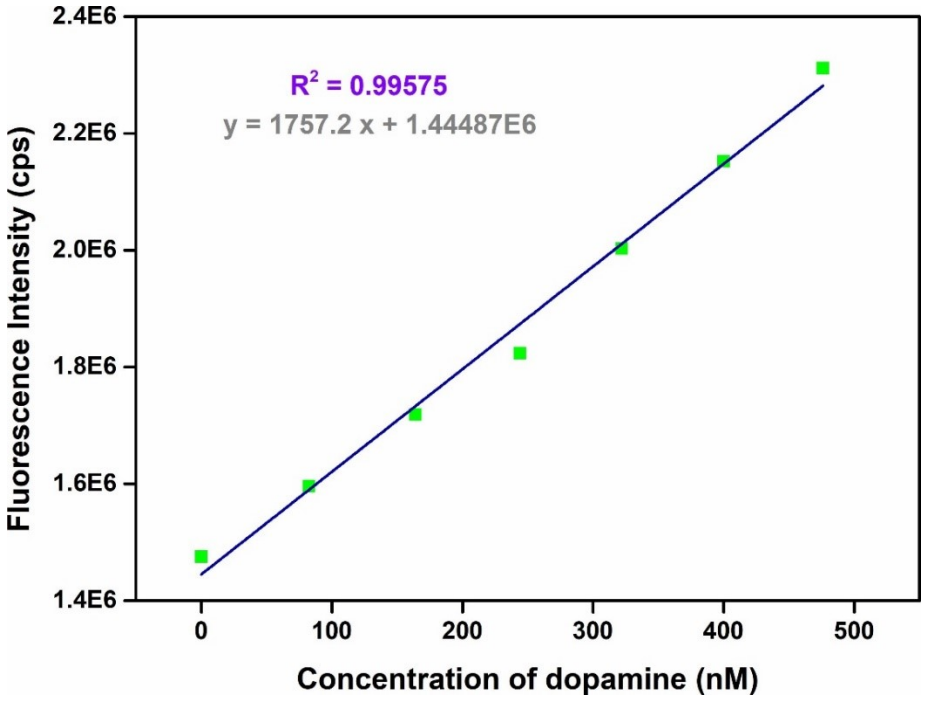

Fig. S36. Change in the fluorescence intensity of **1′** in water as a function of concentration of dopamine.

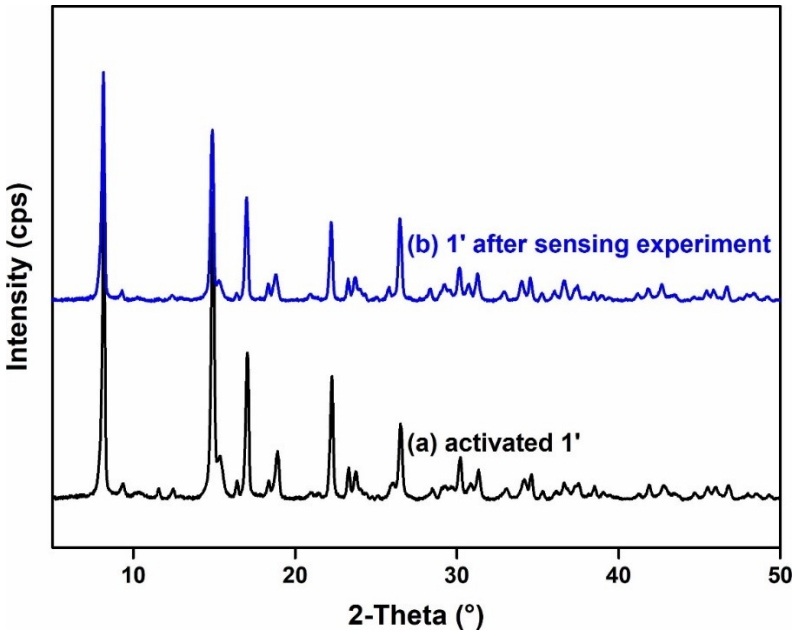

Fig. S37. PXRD patterns of compound **1′** before (a) and after (b) treatment with dopamine in HEPES buffer medium.

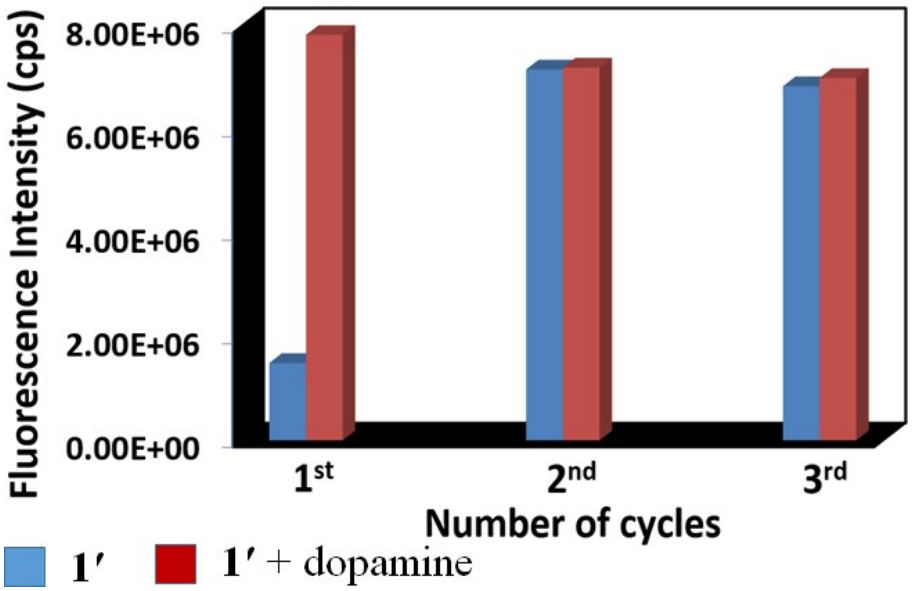

Fig. S38. Recyclability test of **1′** towards the sensing of dopamine in water.

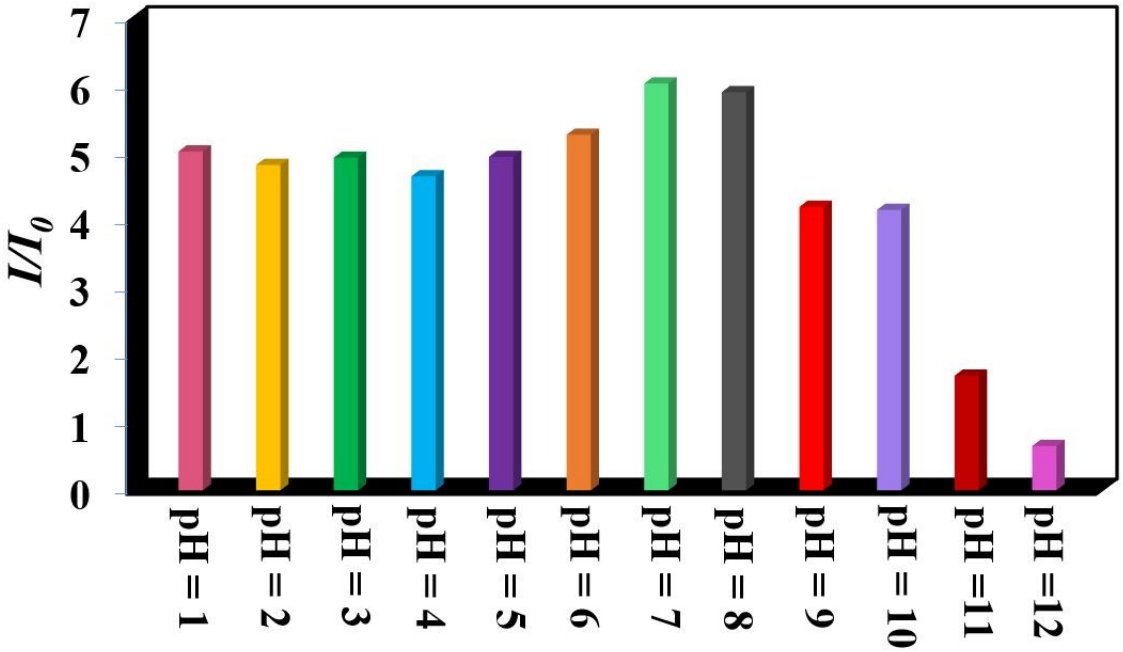

Fig. S39. Fluorescence changes of **1′** after adding 100 μL of 10 mM dopamine solution in different pH solutions (λ_{ex} = 280 nm, λ_{em} = 350 nm).

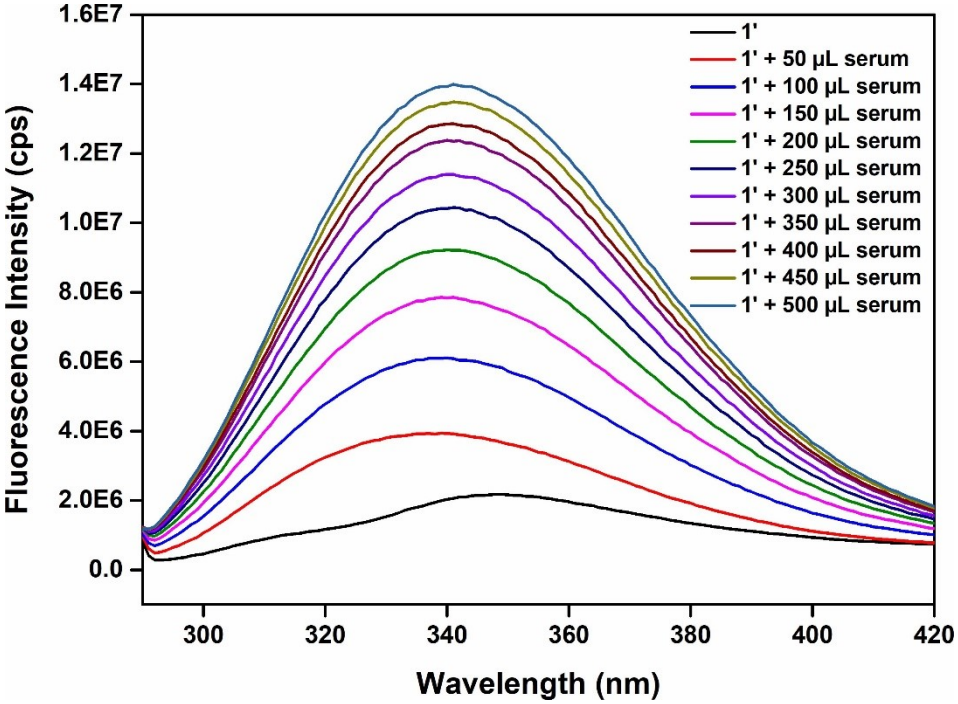

Fig. S40. Turn-on in fluorescence emission intensity of the suspension of **1′** in HEPES buffer medium after addition of 10 mM of different volumes of dopamine-spiked serum solution.

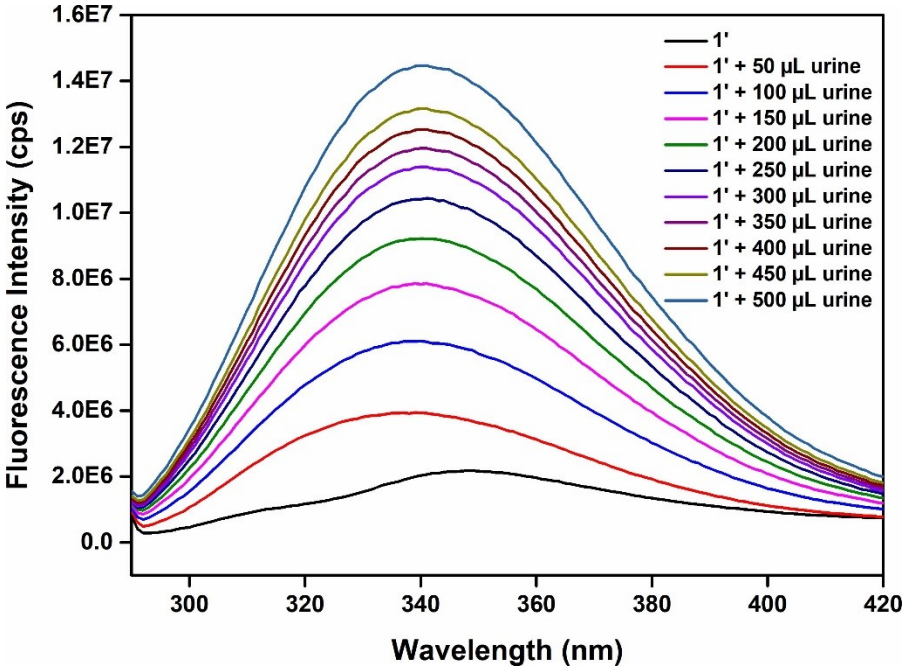

Fig. S41. Turn-on in fluorescence emission intensity of the suspension of **1′** in HEPES buffer medium after addition of 10 mM different volumes of dopamine-spiked urine solution.

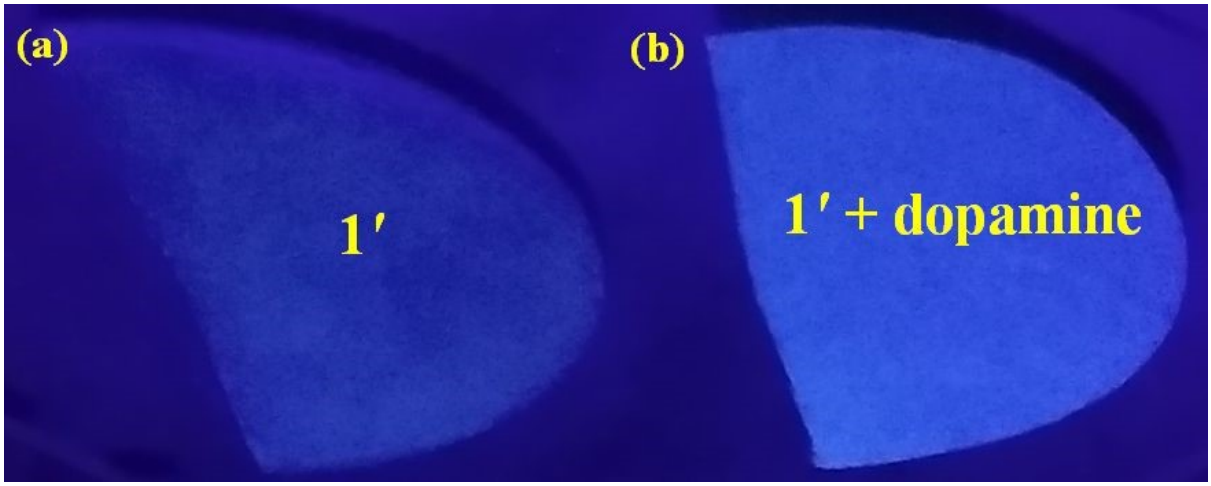

Fig. S42. Images of **1′**-coated paper strips under UV lamp (a) before and (b) after treatment with dopamine solution.

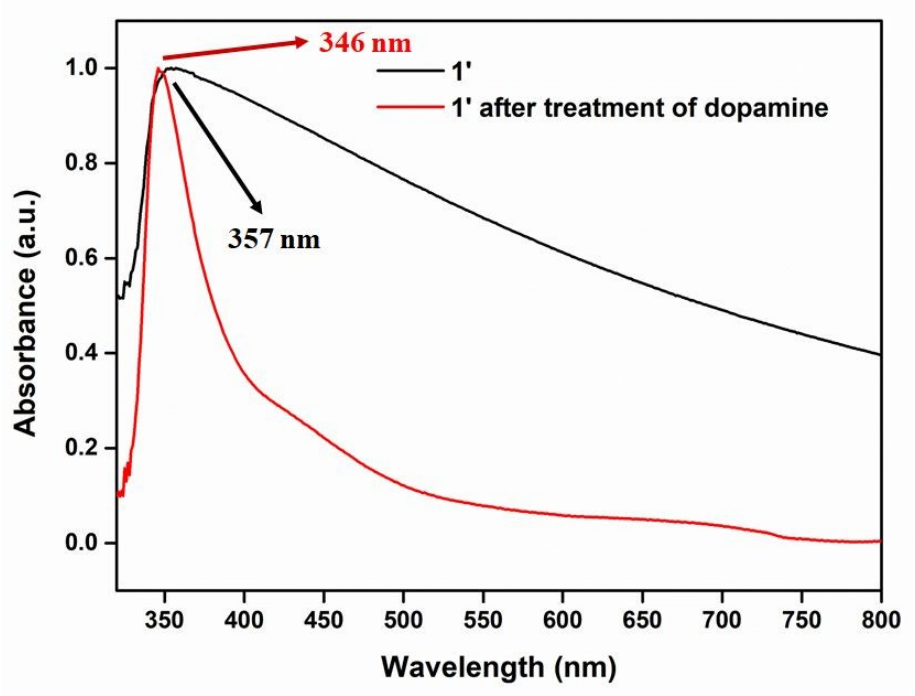

Fig. S43. UV-Vis spectra of compound **1′** in absence (black) and presence (red) of dopamine solution (100 µL, 10 mM).

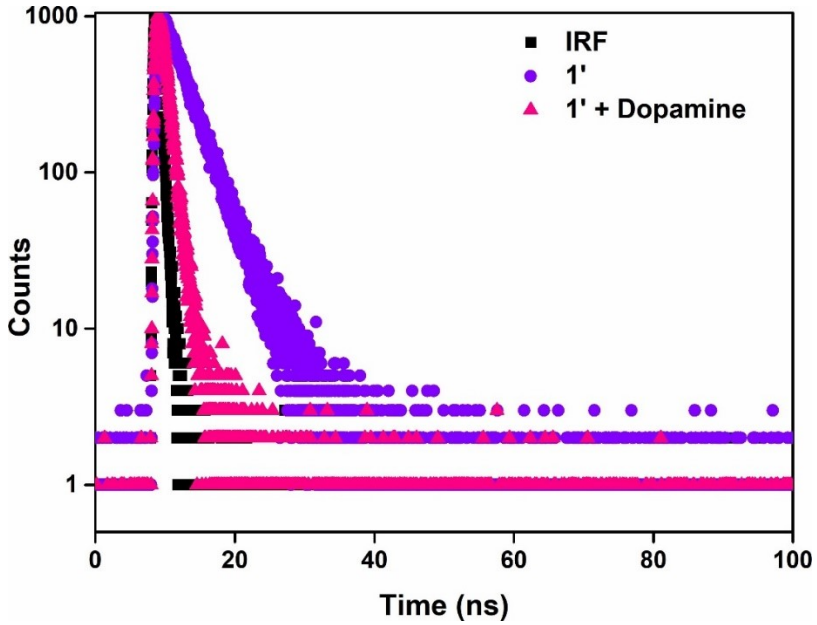

Fig. S44. Lifetime decay profile of **1′** in absence and presence of dopamine solution (λ_{ex} = 280 nm, monitored at 290 nm).

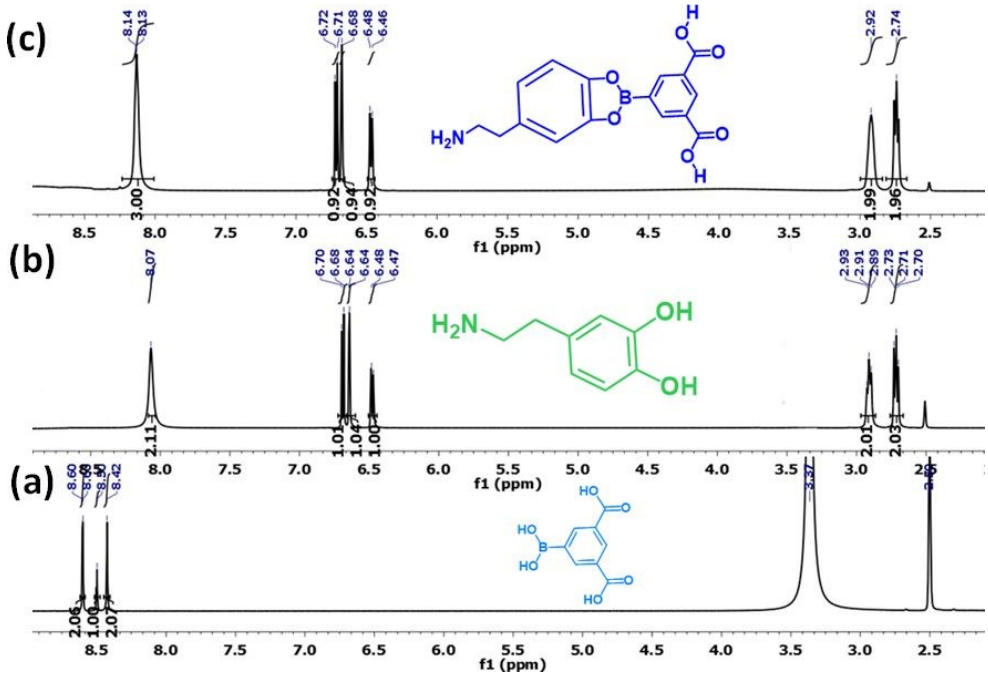

Fig. S45. (a) ^{1}H NMR spectra of the free linker molecule, (b) free dopamine and (c) the linker obtained after the treatment with dopamine in DMSO-d_6 medium. In case of dopamine treated sample, except the dopamine protons, no other additional peaks were found. But, the peaks corresponding to the linker molecules are shifted towards the up-field region (peaks at 8.60 and 8.50 are shifted to 8.14 and 8.13 ppm) and the peak corresponding to the free –OH groups (8.42 ppm) are vanished. Such shift in ^{1}H NMR and the vanishing of –OH protons peak confirm about the complex formation of the linker with dopamine.

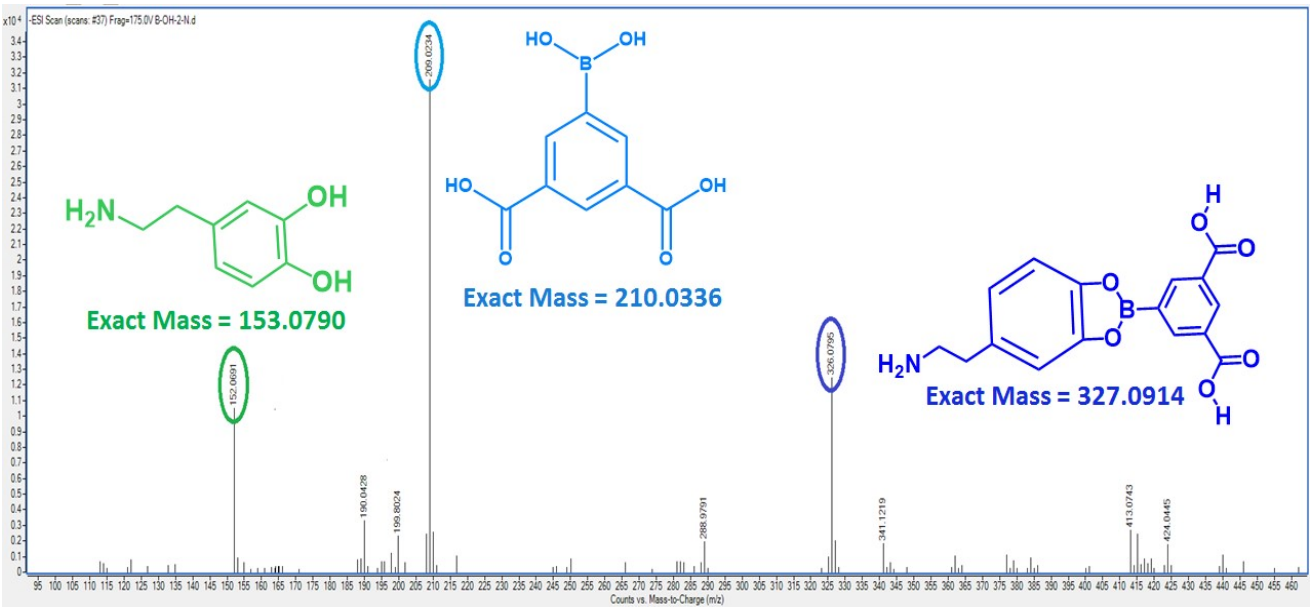

Fig. S46. ESI-MS spectrum of dopamine-treated 5-boronoisophthalic acid linker showing m/z (negative ion mode) peaks at 152.0089, 209.0231, and 327.0914 which correspond to $(M-H)^-$ ion of free dopamine, free linker and dopamine coordinated linker respectively.

Spectral data	Product
Molecular weight of $C_{14}H_{16}N_2O_3$ found: 260.2 Exact mass of GC-MS found m/z: 260.1 **(Fig. S47)** Purification by column chromatography, eluent: hexane/ethyl acetate 65:35. ^{1}H NMR ($CDCl_3$, 400 MHz): δ = 7.03-7.16 (m, 6H), 4.92 (s, 1H), 4.00 (q, J = 7.2 Hz. 2H), 2.25 (s, 3H), 1.09 (t, J = 7.2 Hz. 3H). **(Fig. S48)**	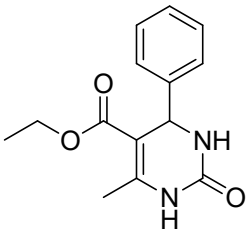
Molecular weight of $C_{14}H_{15}FN_2O_3$ found: 278.2 Exact mass of GC-MS found m/z: 278.1 **(Fig. S49)** Purification by column chromatography, eluent: hexane/ethyl acetate 65:35. ^{1}H NMR (DMSO-d6, 400 MHz): δ =9.18 (s, 1H), 7.71(s, 1H), 7.25 (d, J= 8.4 Hz. 2H), 7.13(d, J=8.7 Hz. 2H). 5.15 (s, 1H), 3.98 (q, J=7.2 Hz. 2H), 2.25(s, 3H), 1.08 (t, J=7.2 Hz. 3H). **(Fig. S50)**	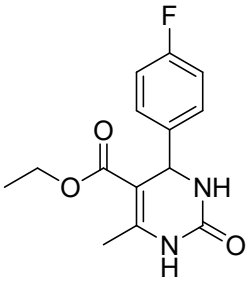

Molecular weight of $C_{14}H_{15}ClN_2O_3$ found: 294.2 Exact mass of GC-MS found m/z: 294.1 **(Fig. S51)** Purification by column chromatography, eluent: hexane/ethyl acetate 65:35. ^{1}H NMR (DMSO-d6, 400 MHz): δ =9.20 (s, 1H), 7.73(s, 1H), 7.38(d, J= 8.4 Hz. 2H), 7.24(d, J=8.7 Hz. 2H). 5.15 (s, 1H), 3.97 (q, J=7.2 Hz. 2H), 2.25(s, 3H), 1.09 (t, J=7.2 Hz.3H). **(Fig. S52)**	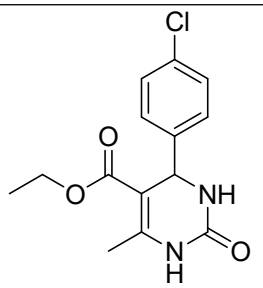
Molecular weight of $C_{14}H_{15}BrN_2O_3$ found: 339.1 Exact mass of GC-MS found m/z: 338.0 **(Fig. S53)** Purification by column chromatography, eluent: hexane/ethyl acetate 65:35. ^{1}H NMR (DMSO-d6, 400 MHz): δ =9.22 (s, 1H), 7.95(s, 1H), 7.50(d, J= 8.4 Hz. 2H), 7.16(d, J=8.7 Hz. 2H). 5.12 (s, 1H), 3.94 (q, J=7.2 Hz. 2H), 2.25(s, 3H), 1.06 (t, J=7.2 Hz.3H). **(Fig. S54)**	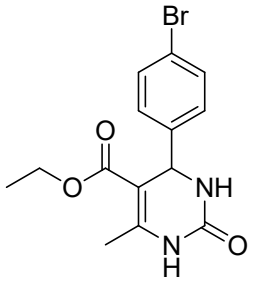
Molecular weight of $C_{14}H_{15}N_3O_5$ found: 305.2 Exact mass of GC-MS found m/z: 305.1 **(Fig. S55)** Purification by column chromatography, eluent: hexane/ethyl acetate 65:35. ^{1}H NMR (DMSO-d6, 400 MHz): δ =9.25 (s, 1H), 7.83 (d, J=7.2 Hz. 1H) 7.67(s, 1H), 7.49(m, 2H), 7.44(t, J=7.2 Hz. 1H). 5.33 (s, 1H), 3.96 (q, J=6.9Hz. 2H), 2.29 (s, 3H), 1.06 (t, J=6.9 Hz.3H). **(Fig. S56)**	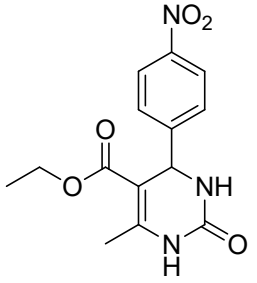
Molecular weight of $C_{15}H_{18}N_2O_4$ found: 290.3 Exact mass of GC-MS found m/z: 290.01 **(Fig. S57)** Purification by column chromatography, eluent: hexane/ethyl acetate 65:35. δ = 9.5 (s, 1H), 7.12 (d, J = 8.4 Hz, 2H), 6.89 (d, J = 8.7 Hz, 3H), 5.11 (s, 1H); 4.00 (q, J = 7.2 Hz, 2H); 3.73 (s, 3H); 2.29 (s, 3H); 1.09 (t, J = 7.2, Hz, 3H). **(Fig. S58)**	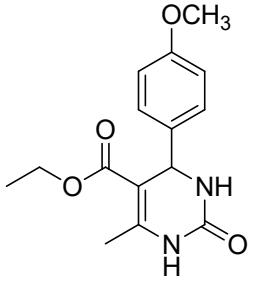

Molecular weight of $C_{14}H_{16}N_2O_4$ found: 276.2 Exact mass of GC-MS found m/z: 276.01 **(Fig. S59)** Purification by column chromatography, eluent: hexane/ethyl acetate 65:35. ^{1}H NMR (DMSO-d6, 400 MHz): δ = 9.34 (s, 1H), 9.10 (s, 1H), 7.61 (s, 1H), 7.02 (d, J = 7.8 Hz. 2H), 6.68 (m, 2H) 5.04 (s, 1H) 3.95 (q, J = 7.2 Hz, 2H) 2.24 (s, 3H) 1.08 (t, J = 7.2 Hz. 3H) **(Fig. S60).**	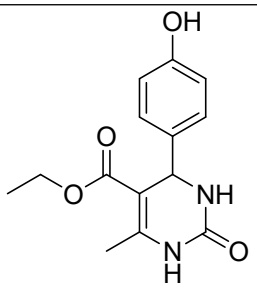
Molecular weight of $C_{15}H_{18}N_2O_3$ found: 275.2 Exact mass of GC-MS found m/z: 275.1 **(Fig. S61)**	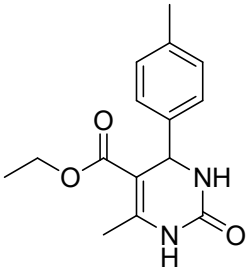
Molecular weight of $C_{18}H_{18}N_2O_3$ found: 310.3 Exact mass of GC-MS found m/z: 310.3 **(Fig. S62)**	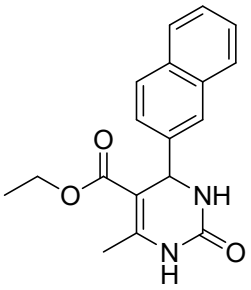

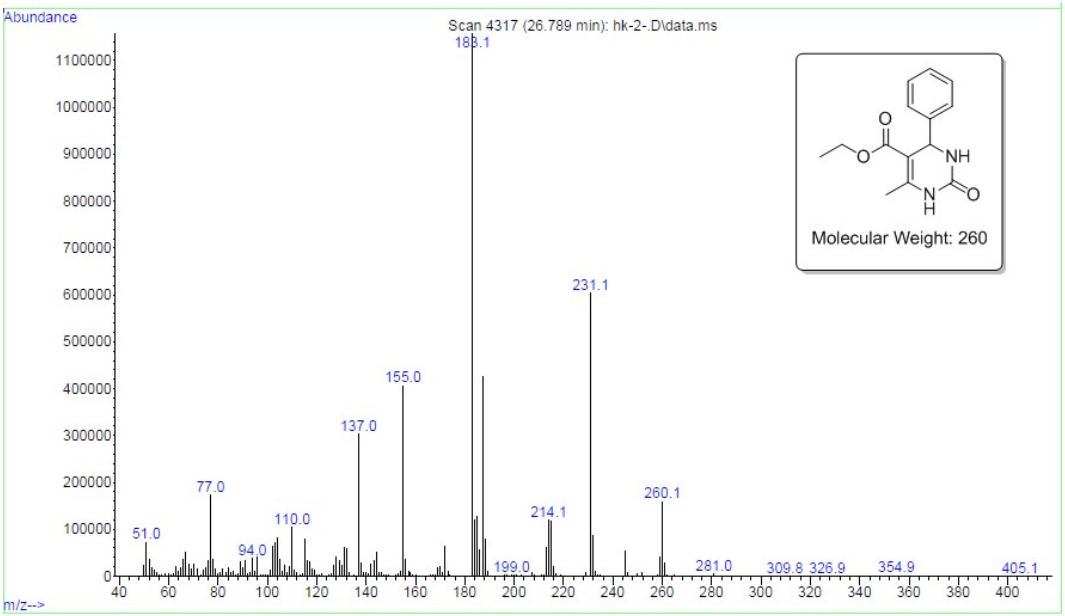

Fig. S47. GC-MS trace of ethyl 6-methyl-2-oxo-4-phenyl-1,2,3,4-tetrahydropyrimidine-5-carboxylate.

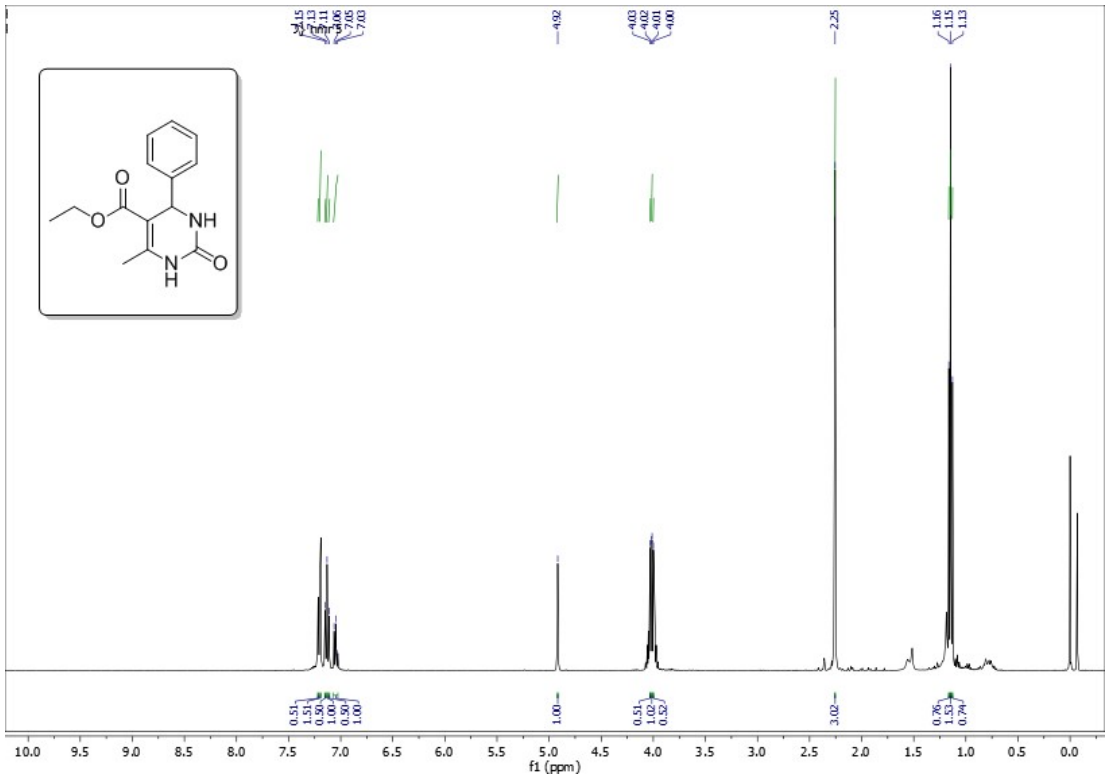

Fig. S48. The [1]HNMR spectrum of ethyl 6-methyl-2-oxo-4-phenyl-1,2,3,4-tetrahydropyrimidine-5-carboxylate.

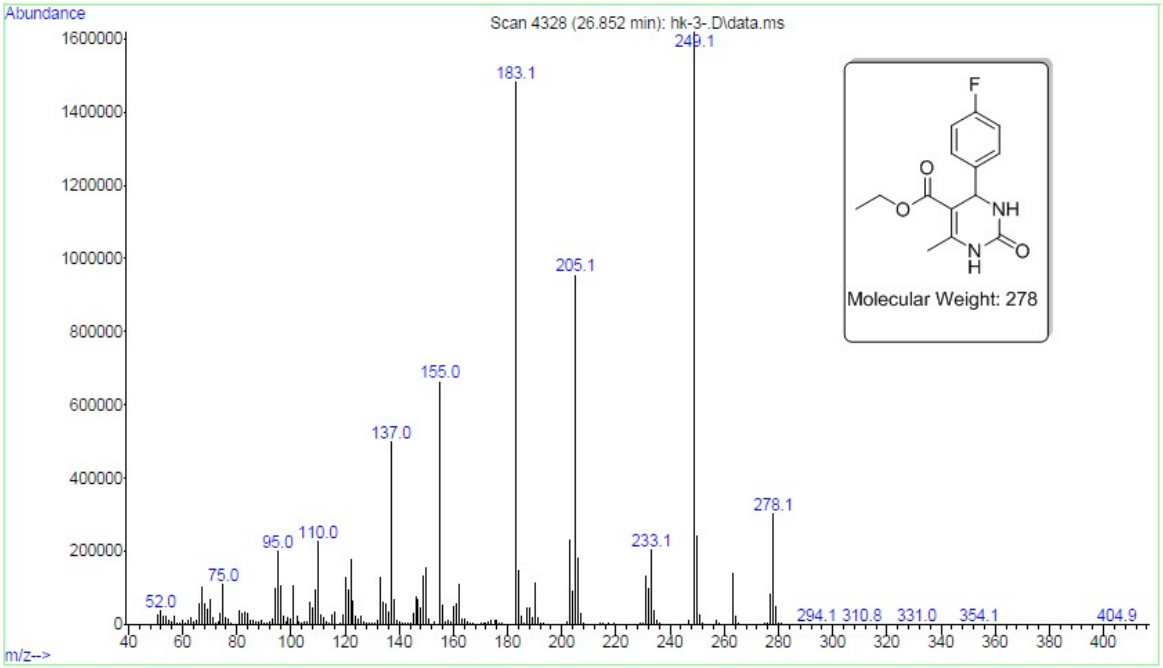

Fig. S49. GC-MS trace of ethyl4-(4-fluorophenyl)-6-methyl-2-oxo-1,2,3,4-tetrahydropyrimidine-5-carboxylate.

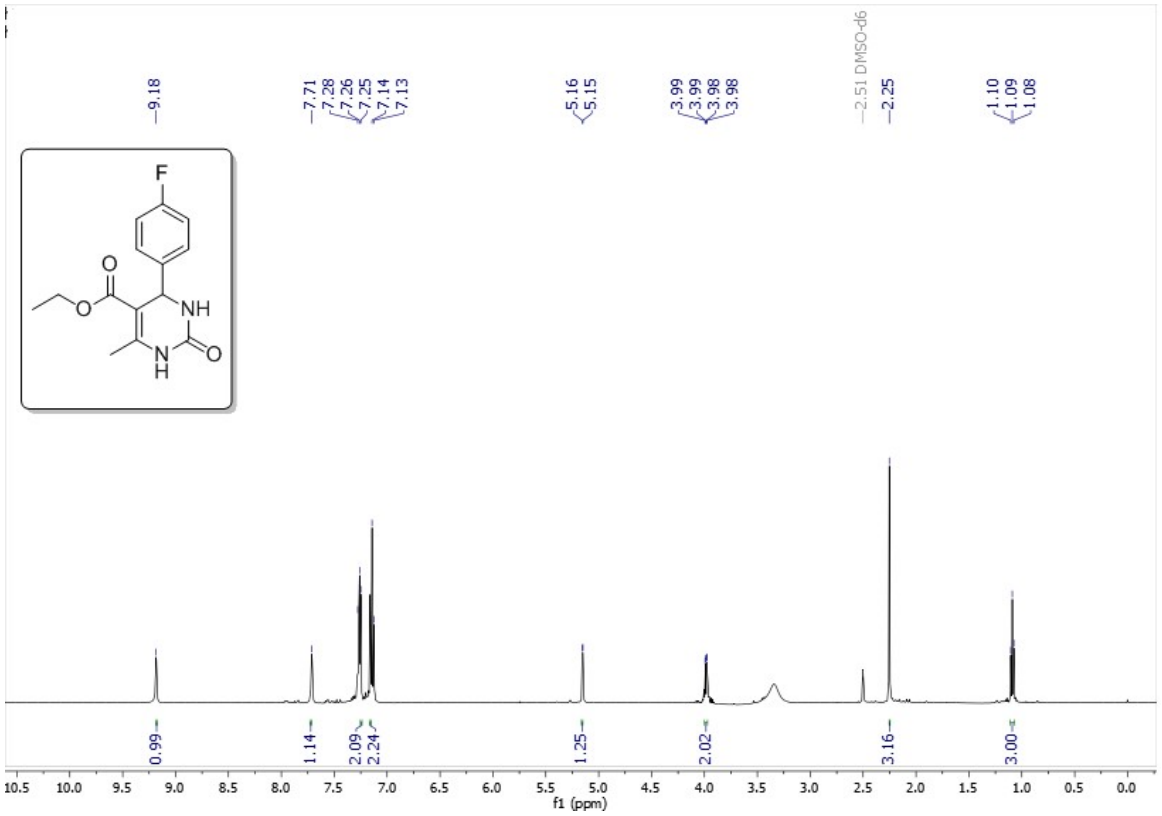

Fig. S50. The [1]HNMR spectrum of ethyl 4-(4-fluorophenyl)-6-methyl-2-oxo-1,2,3,4-tetrahydropyrimidine-5-carboxylate.

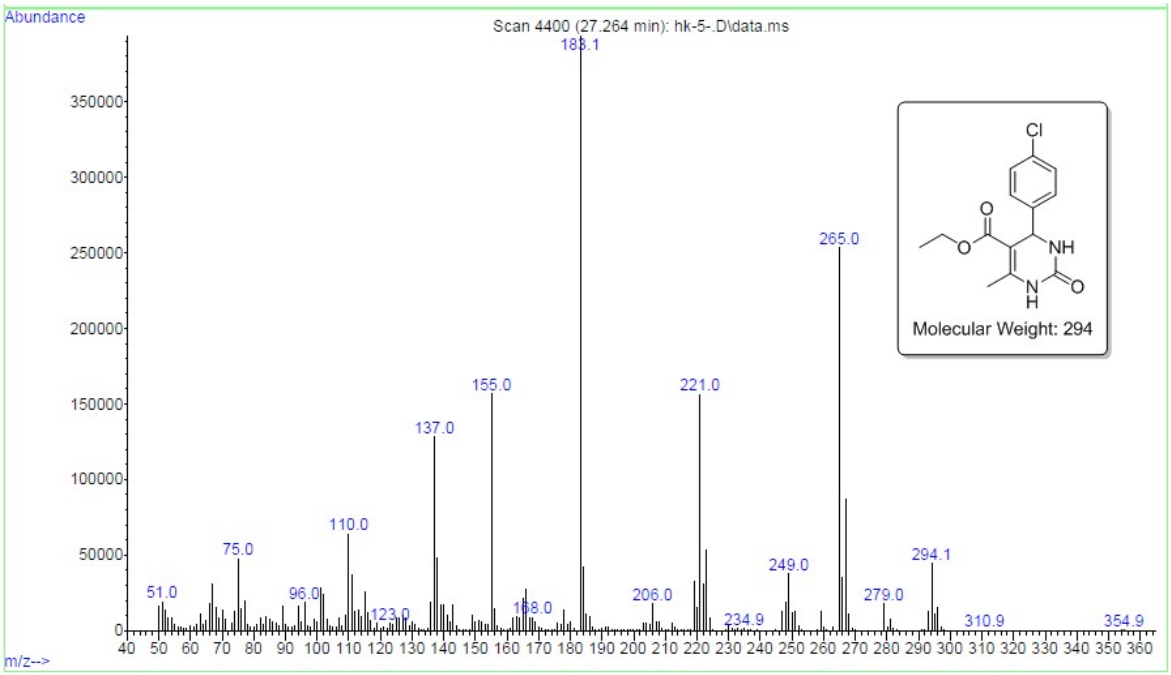

Fig. S51. GC-MS trace of ethyl 4-(4-chlorophenyl)-6-methyl-2-oxo-1,2,3,4-tetrahydropyrimidine-5-carboxylate.

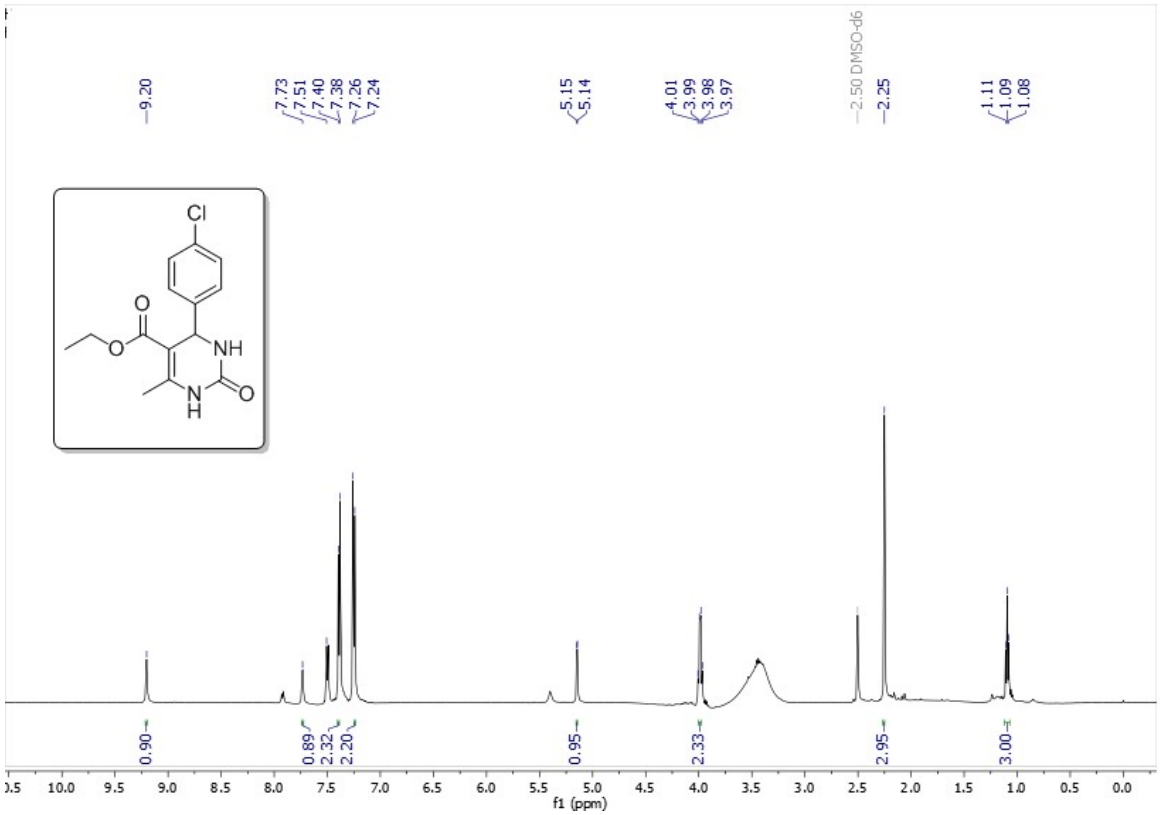

Fig. S52. The [1]HNMR spectrum of ethyl 4-(4-chlorophenyl)-6-methyl-2-oxo-1,2,3,4-tetrahydropyrimidine-5-carboxylate.

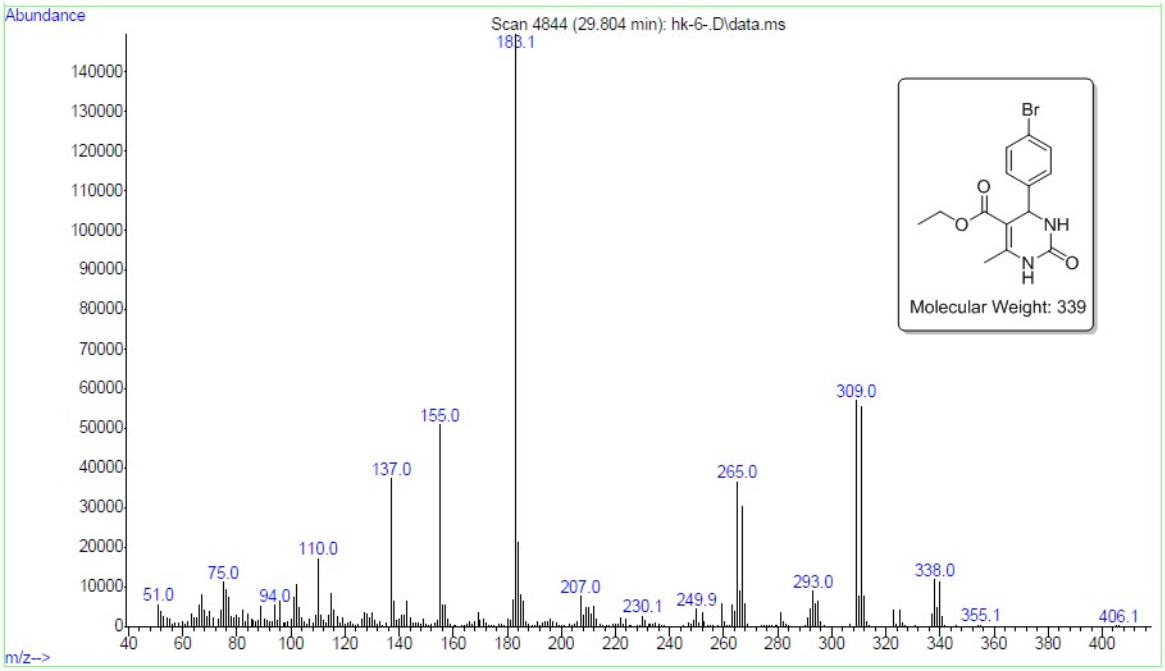

Fig. S53. GC-MS trace of ethyl4-(4-bromophenyl)-6-methyl-2-oxo-1,2,3,4-tetrahydropyrimidine-5-carboxylate.

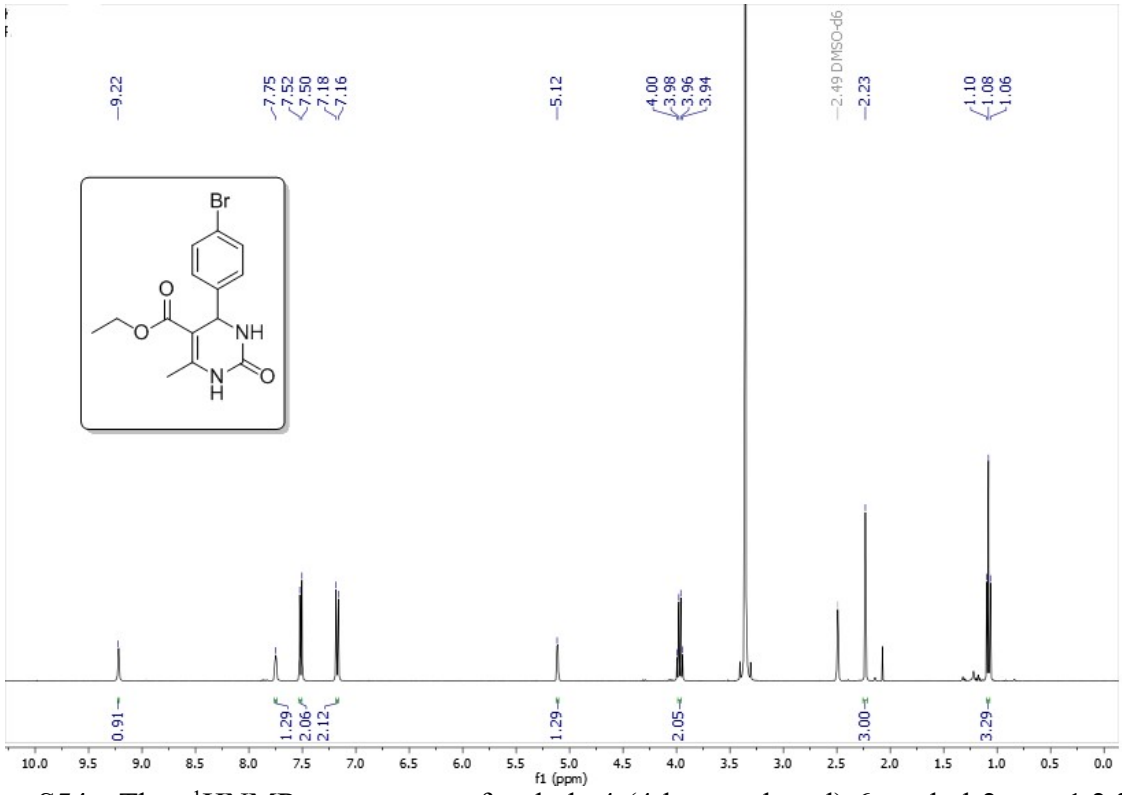

Fig. S54. The ^{1}HNMR spectrum of ethyl 4-(4-bromophenyl)-6-methyl-2-oxo-1,2,3,4-tetrahydropyrimidine 5-carboxylate.

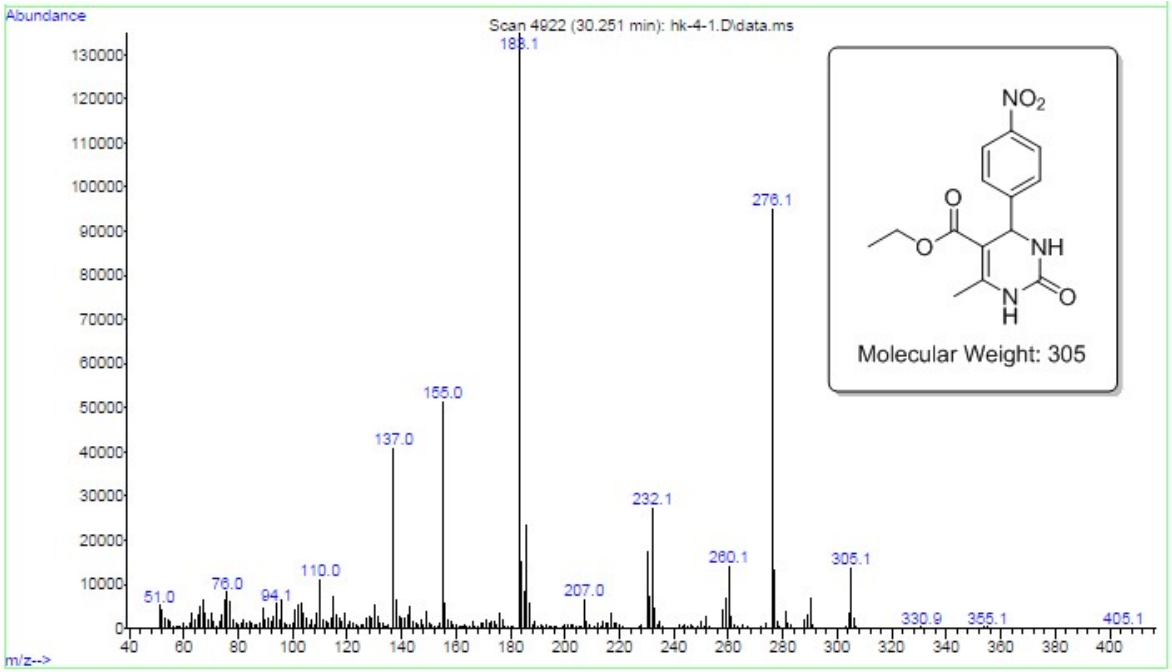

Fig. S55. GC-MS trace of ethyl6-methyl-4-(4-nitrophenyl)-2-oxo-1,2,3,4-tetrahydropyrimidine-5-carboxylate.

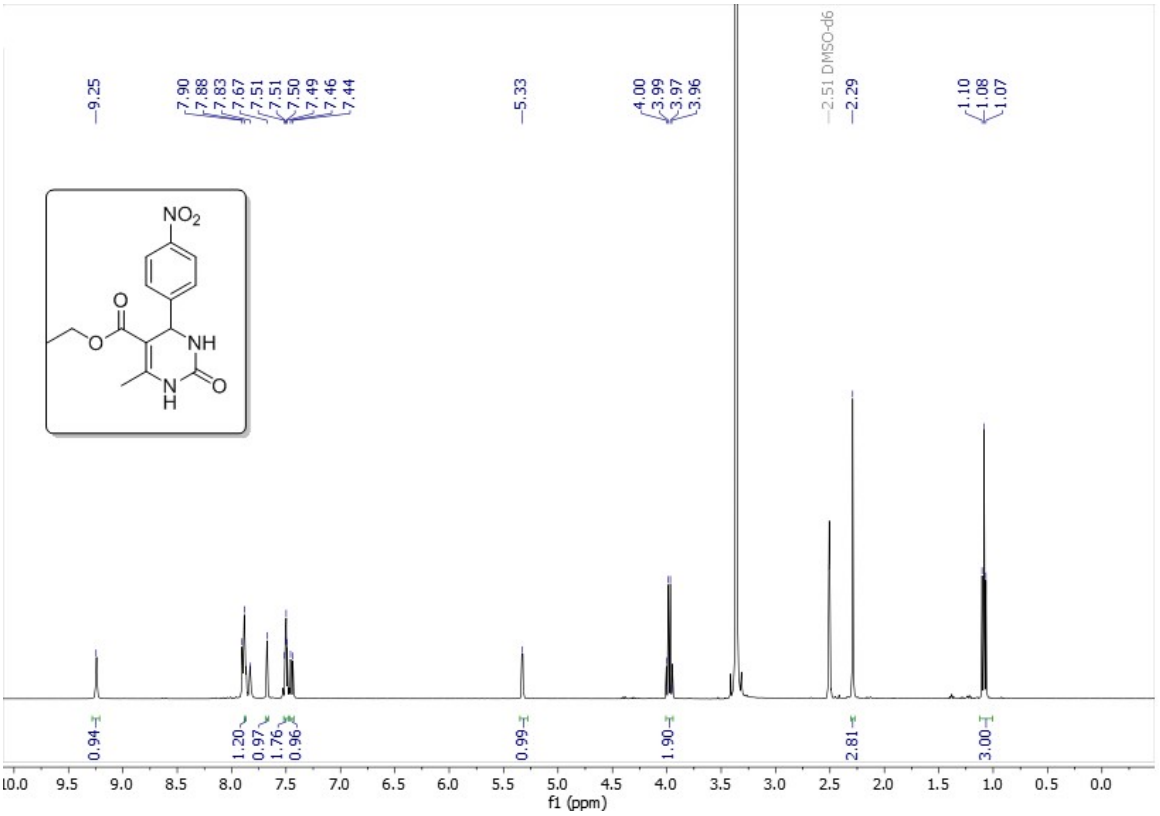

Fig. S56. The [1]HNMR spectrum of ethyl6-methyl-4-(4-nitrophenyl)-2-oxo-1,2,3,4-tetrahydropyrimidine-5-carboxylate.

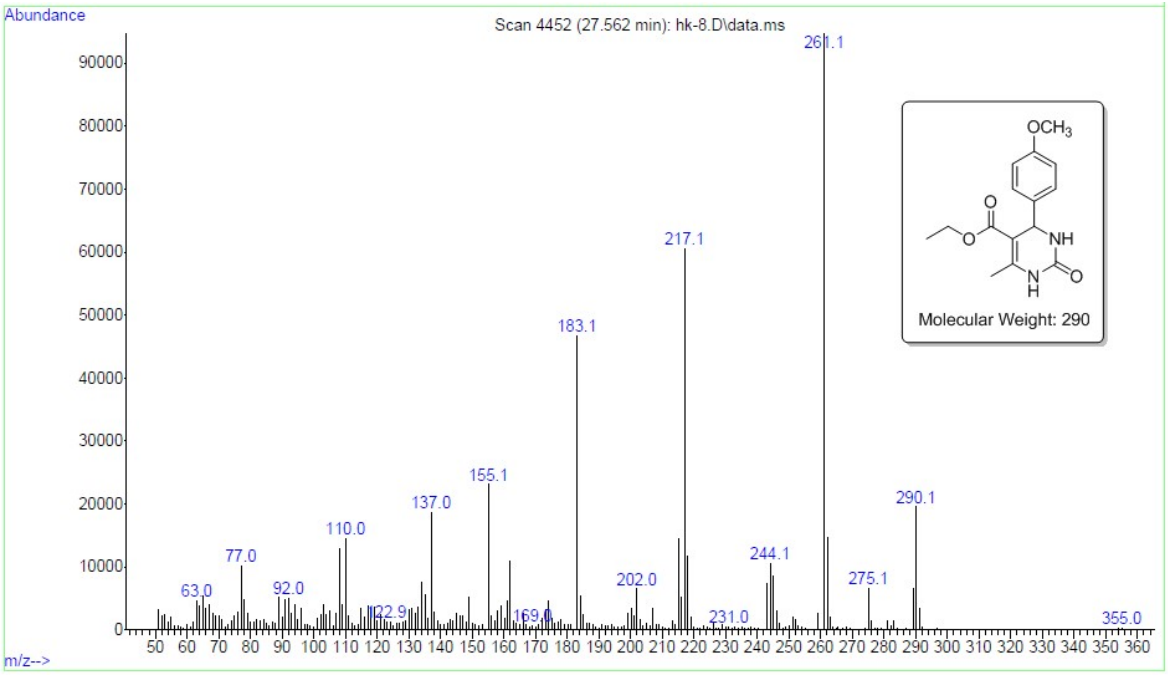

Fig. S57. GC-MS trace of ethyl 4-(4-methoxyphenyl)-6-methyl-2-oxo-1,2,3,4-tetrahydropyrimidine-5-carboxylate.

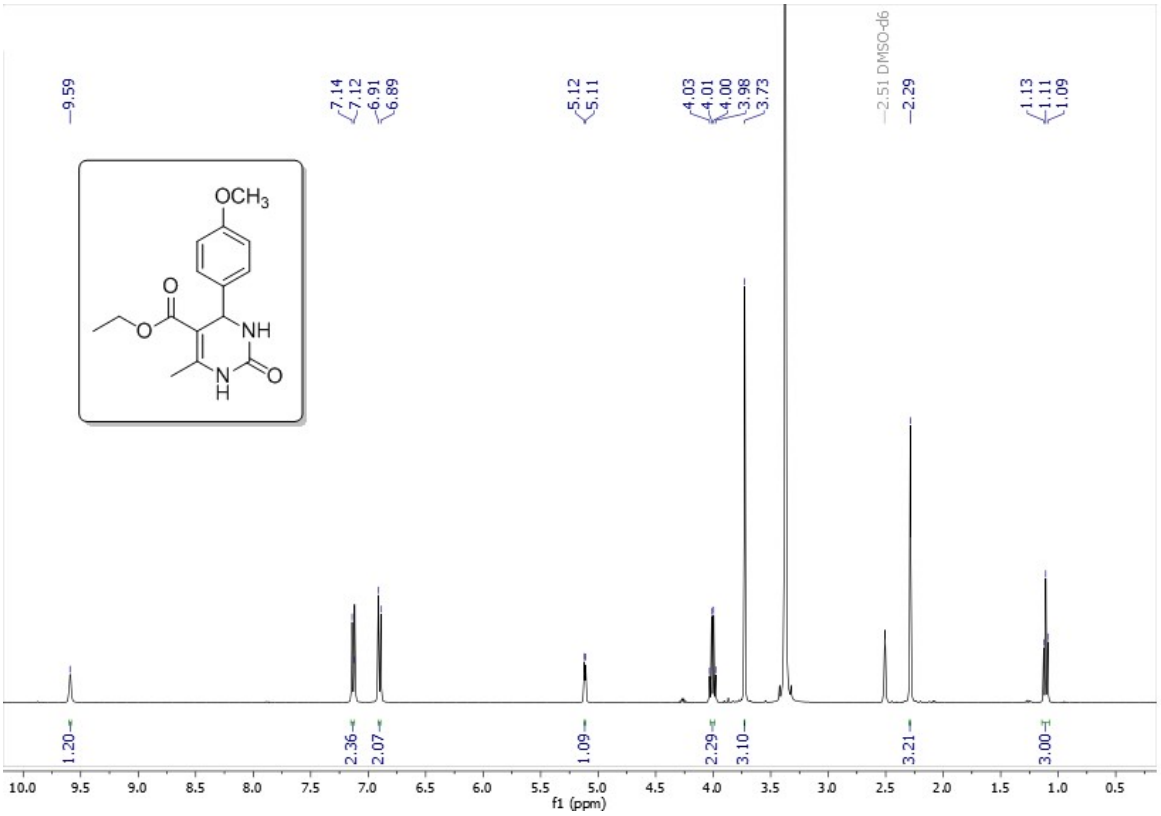

Fig. S58. The [1]HNMR spectrum of ethyl 4-(4-methoxyphenyl)-6-methyl-2-oxo-1,2,3,4-tetrahydropyrimidine-5-carboxylate.

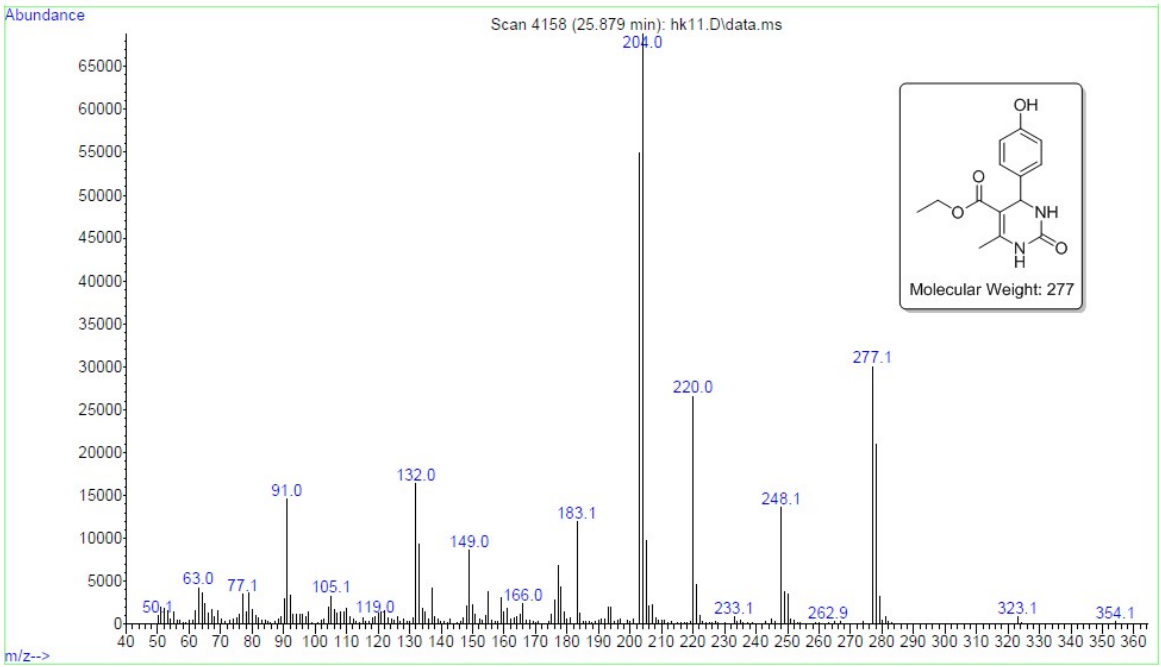

Fig. S59. GC-MS trace of ethyl 4-(4-hydroxyphenyl)-6-methyl-2-oxo-1,2,3,4-tetrahydropyrimidine-5-carboxylate.

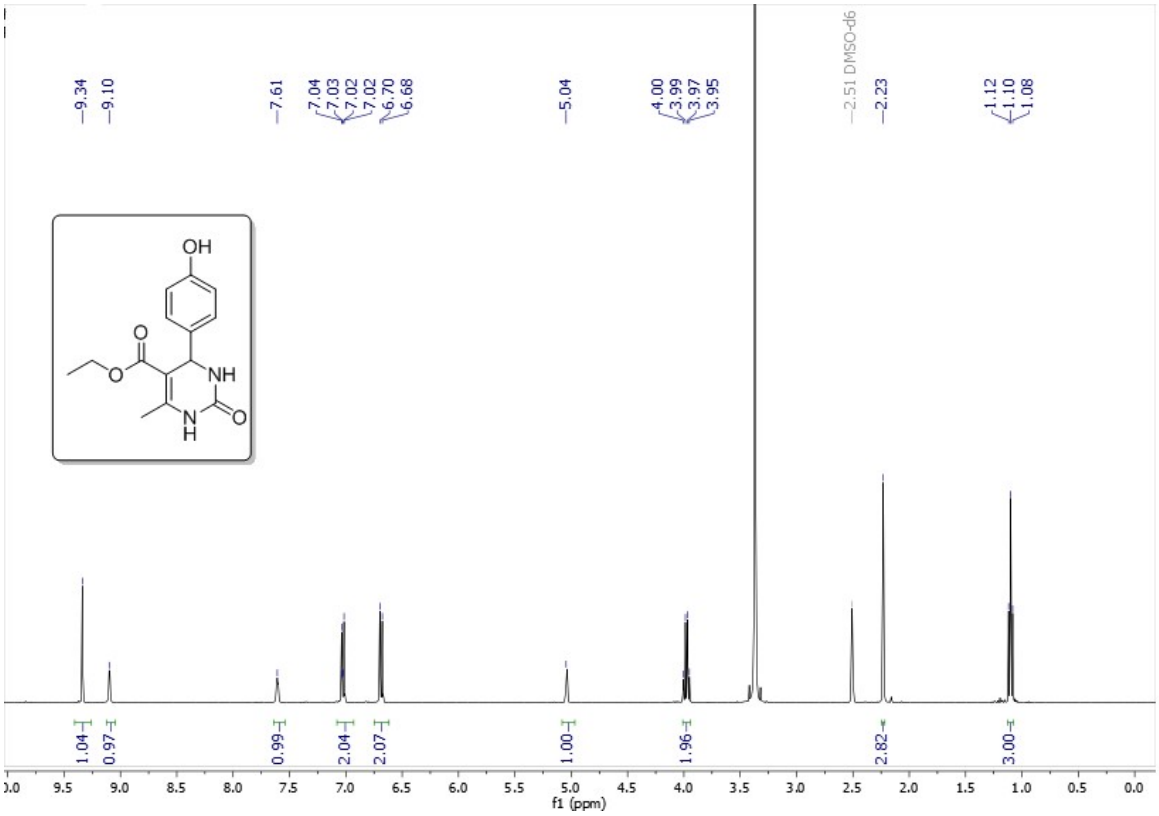

Fig. S60. The [1]HNMR spectrum of ethyl4-(4-hydroxyphenyl)-6-methyl-2-oxo-1,2,3,4-tetrahydropyrimidine-5-carboxylate.

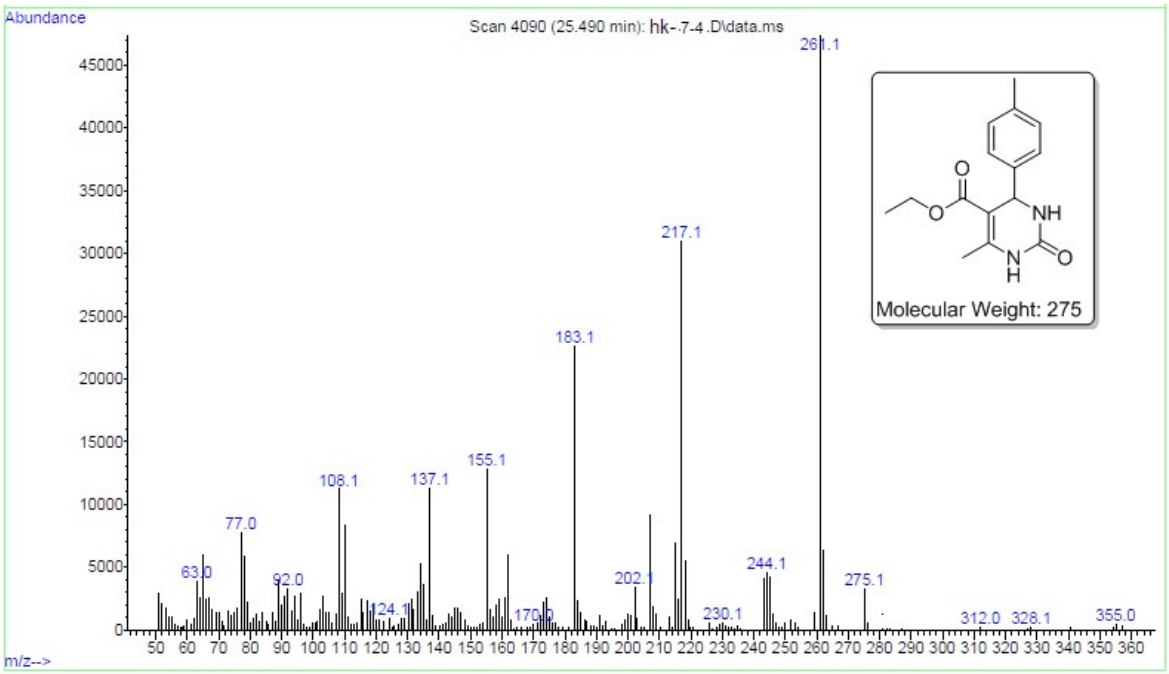

Fig. S61. GC-MS trace of ethyl 6-methyl-2-oxo-4-(p-tolyl)-1,2,3,4-tetrahydropyrimidine-5-carboxylate.

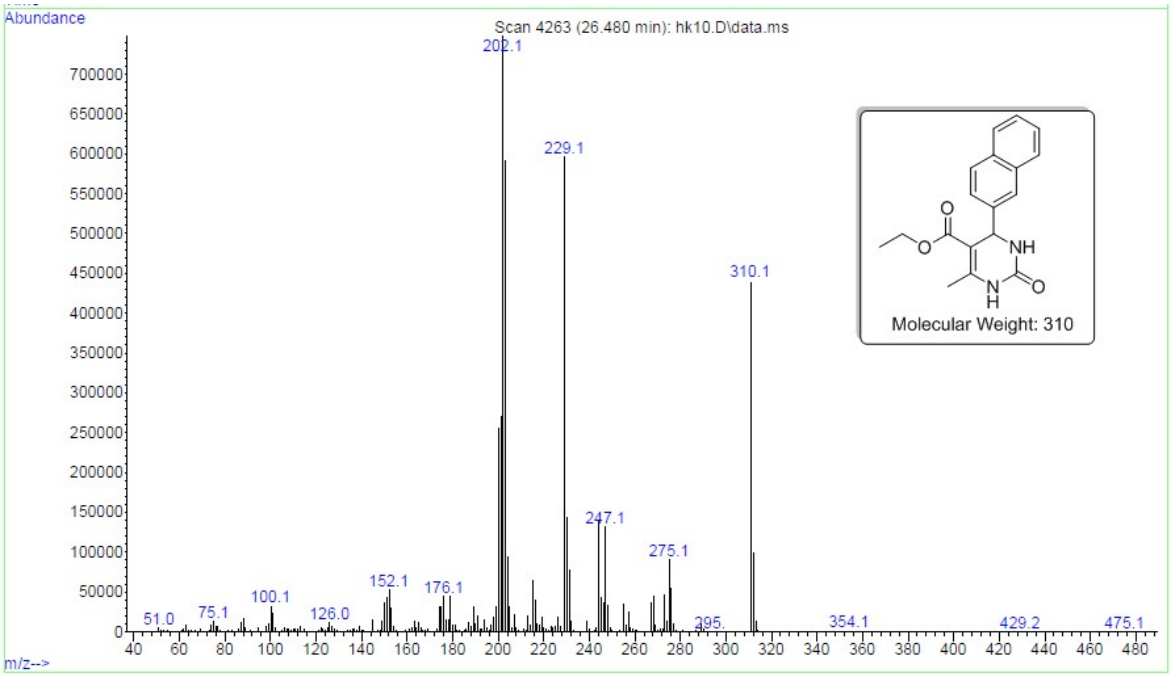

Fig. S62. GC-MS trace of ethyl 6-methyl-4-(naphthalen-2-yl)-2-oxo-1,2,3,4-tetrahydropyrimidine-5-carboxylate.

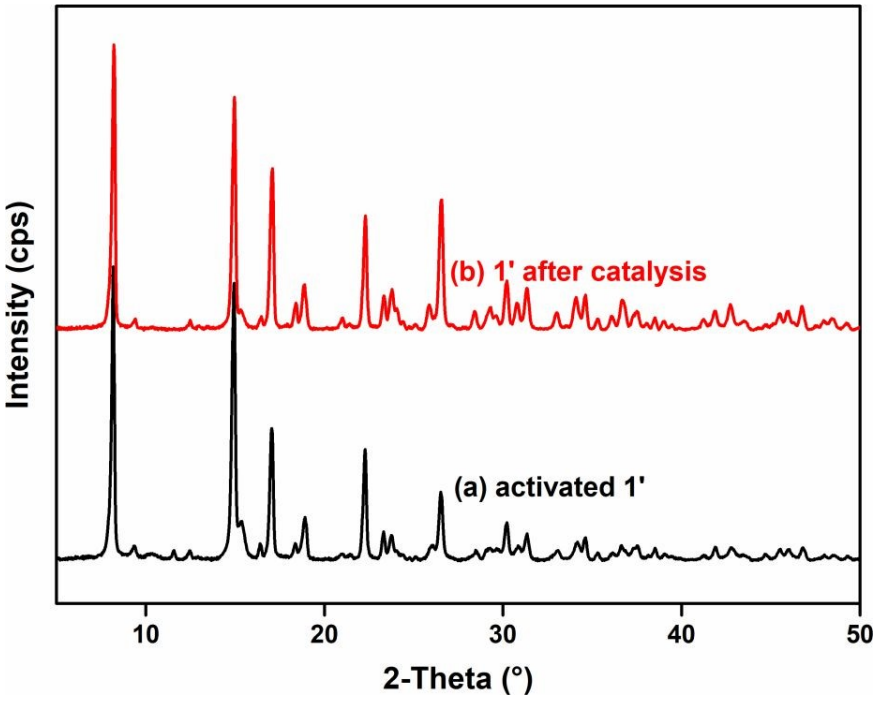

Fig. S63. PXRD patterns of (a) fresh and (b) three times reused **1′**.

Table S1. Results of the structure-less Pawley refinements.

	CAU-10-B(OH)$_2$
space group	$I4_1md$
$a = b$ [Å]	21.5762(8)
c [Å]	10.4567(6)
$\alpha = \beta = \gamma$ [°]	90
R_{WP} [%]	4.5
GoF	3.2

Table S2. Comparison of the response time, detection limit and sensing media used for the reported chemosensors of dopamine in the literature.

Sl. No.	Sensor Material	Type of Material	Sensing Medium	Detection Limit	Response Time	Detection method	Ref.
1	$Cu_3(HHPT)_2$	MOF	0.1 M $CaCl_2$ solution	100 nM	-	Electrochemical	2
2	AgPd@Zr-MOF	MOF	-	0.1 µM	-	Electrochemical	3
3	Organic molecule	Organic molecule	Alkali medium	0.3 µM	30 min	Fluorescence	4
4	CDs	CDs	Aqueous	20 nM	-	Fluorescence	5
5	BA-Tb-MOG	Metal-organic gel	Aqueous	0.08 µM	0.5 min	Fluorescence	6
6	Gold template	Polymer film	Aqueous	200 nM	-	Electrochemical	7
7	Aptamer-modified electrodes	Gold electrodes	-	20 nM	-	Electrochemical	8
8	EµPAN	Chromatography paper	5 mM K3[Fe(CN)6] in 0.5 M KCl	0.01 µM	-	Electrochemical	9
9	ECP	Ultrathin metal−organic nanosheets	PBS-buffer	21 nM	5 min	Fluorescence	10
10	N-GQDs	Quantum dots	PBS-buffer	0.07 mM	40 min	Fluorescence	11
11	Abtz–CdI_2–MOF	MOF	0.1 M Tris–HCl buffer	57 nM	10 min	Fluorescence	12
12	Eu-MOF	MOF	1.0 mL PBS	0.015 mM	1 min	Fluorescence	13

13	CNT-N	Carbon nanotube	-	1 μM to 20 μM	15 min	Electrochemical	14
14	Polydopamine nanoparticles	-	PBS-buffer NaOH and HCl	40 nM	3 h	Fluorescence	15
15	[Al(OH)(IPA-$B(OH)_2$)]·$1H_2O$· 0.5DMF (**1′**)	MOF	HEPES-buffer H_2O	3.5 nM 11.7 nM	<1 min	Fluorescence	this work

Table S3. Fluorescence lifetimes of **1′** before and after the addition of dopamine solution (λ_{ex} = 320 nm, pulsed diode laser).

Volume of dopamine solution added (μL)	a_1	a_2	τ_1 (ns)	τ_2 (ns)	$<\tau>$* (ns)
0	0.88	0.12	3.07	5.96	3.42
100	0.95	0.5	0.78	3.16	2.32

* $<\tau> = a_1\tau_1 + a_2\tau_2$

Table S4. Comparison of the activity of **1′** with other catalysts for the Biginelli reaction.

Entry	Catalyst	T (°C)	Time (h)	Yield (%)	Ref.
1	PTA@MIL-101	100	1	90	16
2	Cu-based MOF	60	2	86	17
3	IRMOF-3	60	7	93	18
4	Zn-based MOF	60	2	93	19
5	$[Co(DPP)_2(H_2O)_2]\cdot(BS)_2 2H_2O$	80	2	85	20
6	$TiCl_4$-$MgCl_2\cdot 4CH_3OH$	100	3	90	21
7	Ni-DDIA MOF	80	0.5	84.6	22
8	$Cu(INA)_2$.MOF	80	2	99	23
9	[Al(OH)(IPA-$B(OH)_2$)] ·$1H_2O$·0.5DMF (**1′**)	80	24	94	this work

References:

1. J. Jiang, Q. Wang, M. Zhang and J. Bai, *Cryst. Growth Des.*, 2017, **17**, 2223–2227.
2. J. Song, J. Zheng, A. Yang, H. Liu, Z. Zhao, N. Wang and F. Yan, *Mater. Chem. Front.*, 2021, **5**, 3422-3427.
3. S. A. Hira, S. Nagappan, D. Annasa, Y. A. Kumar and K. H. Park, *Electrochem. commun.*, 2021, **125**, 107012-107019.
4. X. Wei, Z. Zhang and Z. Wang, *Microchem. J.*, 2019, **145**, 55–58s.
5. A. Kumar, A. Kumari, P. Mukherjee, T. Saikia, K. Pal and S. K. Sahu, *Microchem. J.*, 2020, **159**, 105590-105601.

6. Y. Sun, Z. Song, X. Ni, P. Dramou and H. He, *Microchem. J.* , 2021, **169**, 106579-106585.
7. T. Łuczak, *Electrochim. Acta*, 2008, **53**, 5725–5731.
8. E. E. Ferapontova, *Electrochim. Acta*, 2017, **245**, 664–671.
9. A. Manbohia and S. H. Ahmadi, *Sens. Bio-Sens. Res*, 2019, **23**, 100270-100276.
10. F. Moghzi, J. Soleimannejad, E. C. Sañudo and J. Janczak, *ACS Appl. Mater. Interfaces*, 2020, **12**, 44499-44507.
11. X. Chen, N. zheng, S. Chen and Q. Ma, *Anal. Methods*, 2017, **9**, 2246–2251.
12. Y. Cheng, J. Wu, C. Guo, X.-G. Li, B. Ding and Y. Li, *J. Mater. Chem. B*, 2017, **5**, 2524--2535.
13. Q. Du, P. Wu, P. Dramou, R. Chen and H. He, *New J. Chem.*, 2019, **43**, 1291--1298.
14. J. Zhao, W. Zhang, P. Sherrell, J. M. Razal, X.-F. Huang, A. I. Minett and J. Chen, *ACS Appl. Mater. Interfaces*, 2012, **4**, 44−48.
15. A. Yildirim and M. Bayindir, *Anal. Chem.*, 2014, **86**, 5508−5512.
16. M. Saikia, D. Bhuyana and L. Saikiaa, *Appl. Catal., A. 505 (2015) 501*, 2015, **505**, 501-506.
17. T. K. Pal, D. De, S. Senthilkumar, S. Neogi and P. K. Bharadwaj, *Inorg. Chem.*, 2016, **55**, 7835–7842.
18. S. Rostamnia and A. Morsali, *RSC Adv.*, 2014, **4**, 29182-29189.
19. A. Verma, D. De, K. Tomar and P. K. Bharadwaj, *Inorg. Chem.*, 2017, **56**, 9765–9771.
20. J. H. Wang, G. M. Tang, Y. T. Wang, Y. Z. Cui, J. J. Wang and S. W. Ng, *Dalton Trans.*, 2015, **44**, 17829-17840.
21. A. Kumar and R. A. Maurya, *J. Mol. Catal. A: Chem.*, 2007, **53**, 53-56.
22. S.-Y. Zhao, Z.-Y. Chen, N. Wei, L. Liu and Z.-B. Han, *Inorg. Chem.*, 2019, **58**, 7657–7661.
23. J. C. M. Willig, G. Granetto, D. Reginato, F. R. Dutra, E. F. Poruczinski, I. M. d. Oliveira, H. A. Stefani, S. D. d. Campos, E. A. d. Campos, F. Manarin and G. V. Botteselle, *RSC Adv.*, 2020, **10**, 3407-3415.